

AD-A206 801

4

TECHNICAL REPORT BRL-TR-2948

**BRL**

1938 - Serving the Army for Fifty Years - 1988

A LUMPED-PARAMETER CODE FOR REVERSE  
ANNULAR LIQUID PROPELLANT GUNS

DTIC  
ELECTE  
S APR 10 1989 D  
D 03

TERENCE P. COFFEE

DECEMBER 1988

APPROVED FOR PUBLIC RELEASE; DISTRIBUTION UNLIMITED.

U.S. ARMY LABORATORY COMMAND

**BALLISTIC RESEARCH LABORATORY**  
**ABERDEEN PROVING GROUND, MARYLAND**

89 4 07 135

DESTRUCTION NOTICE

Destroy this report when it is no longer needed. DO NOT return it to the originator.

Additional copies of this report may be obtained from the National Technical Information Service, U.S. Department of Commerce, Springfield, VA 22161.

The findings of this report are not to be construed as an official Department of the Army position, unless so designated by other authorized documents.

The use of trade names or manufacturers' names in this report does not constitute indorsement of any commercial product.

**REPORT DOCUMENTATION PAGE**

1a. REPORT SECURITY CLASSIFICATION <b>Unclassified</b>			1b. RESTRICTIVE MARKINGS			
2a. SECURITY CLASSIFICATION AUTHORITY			3. DISTRIBUTION / AVAILABILITY OF REPORT Approved for public release; distribution is unlimited.			
2b. DECLASSIFICATION / DOWNGRADING SCHEDULE			4. PERFORMING ORGANIZATION REPORT NUMBER(S)  <b>BRL-TR-2948</b>			
6a. NAME OF PERFORMING ORGANIZATION  <b>US Army Ballistic Rsch Lab</b>		6b. OFFICE SYMBOL (if applicable)  <b>SLCBB-IB</b>		5. MONITORING ORGANIZATION REPORT NUMBER(S)		
6c. ADDRESS (City, State, and ZIP Code)  <b>Aberdeen Proving Ground, MD 21005-5066</b>			7a. NAME OF MONITORING ORGANIZATION			
8a. NAME OF FUNDING / SPONSORING ORGANIZATION		8b. OFFICE SYMBOL (if applicable)		7b. ADDRESS (City, State, and ZIP Code)		
8c. ADDRESS (City, State, and ZIP Code)			9. PROCUREMENT INSTRUMENT IDENTIFICATION NUMBER			
11. TITLE (Include Security Classification) <b>A LUMPED PARAMETER CODE FOR REVERSE ANNULAR LIQUID PROPELLANT GUNS</b>			10. SOURCE OF FUNDING NUMBERS			
			PROGRAM ELEMENT NO.	PROJECT NO.	TASK NO.	WORK UNIT ACCESSION NO.
12. PERSONAL AUTHOR(S) <b>Coffee, Terence P.</b>						
13a. TYPE OF REPORT <b>TR</b>		13b. TIME COVERED FROM _____ TO _____		14. DATE OF REPORT (Year, Month, Day)		15. PAGE COUNT
16. SUPPLEMENTARY NOTATION						
17. COSATI CODES			18. SUBJECT TERMS (Continue on reverse if necessary and identify by block number)			
FIELD	GROUP	SUB-GROUP	liquid monopropellant propellant injection			
			regenerative gun droplet burning reverse annular gun			
			numerical solution lumped parameter model			
19. ABSTRACT (Continue on reverse if necessary and identify by block number)						
<p>In previous reports, a lumped parameter code for in-line regenerative liquid propellant guns was described.<sup>1,2</sup> This code was based on an earlier model by Gough.<sup>3</sup> The Gough code also covered the case of a traveling charge, which required a one-dimensional model in the gun tube. The new code was totally lumped parameter, and the faster run times made parametric studies simpler. Also, the code was set up in a modular fashion, so that new options could easily be added. A number of options have been added to the code to test various hypotheses about the gun behavior, and various options that did not prove useful were removed.</p> <p>The present report describes a variant of the code for reverse annular liquid propellant (RAP) guns. This code was developed specifically to model the high performance system designed and</p> <p>(continued on reverse)</p>						
20. DISTRIBUTION / AVAILABILITY OF ABSTRACT <input type="checkbox"/> UNCLASSIFIED/UNLIMITED <input checked="" type="checkbox"/> SAME AS RPT. <input type="checkbox"/> DTIC USERS			21. ABSTRACT SECURITY CLASSIFICATION <b>Unclassified</b>			
22a. NAME OF RESPONSIBLE INDIVIDUAL <b>Terence P. Coffee</b>			22b. TELEPHONE (Include Area Code) <b>(301) 278-6169</b>		22c. OFFICE SYMBOL <b>SLCBB-IB-B</b>	

19. ABSTRACT (Con't)

fabricated at General Electric Armament and Electrical Systems Department at Burlington, VT.<sup>4</sup> The original Gough code included the reverse annular piston as one option. However, a more general injection design was required for the new gun system. There were enough differences from the in-line piston system that it was more efficient to have a separate code for the RAP gun.

The governing ordinary differential equations are given for the lumped parameter model of a reverse annular regenerative liquid gun. The different options and assumptions are described. The equations are solved numerically using EPISODE, an efficient and robust computer code for the integration of ordinary differential equations.

The code is compared to the experimental gun firings of the GE test fixture. The process of choosing reasonable input parameters is discussed. Problems that occurred in the test firings are analyzed.

### ACKNOWLEDGEMENT

I would like to thank Cris Watson, BRL, for his help in understanding the gun fixture and the experimental data and in obtaining accurate values for the code input parameters.

Accesion For	
NTIS CRA&I	<input checked="" type="checkbox"/>
DTIC TAB	<input type="checkbox"/>
Unannounced	<input type="checkbox"/>
Justification .....	
By .....	
Distribution /	
Availability Codes	
Dist	Avail and/or Special
A-1	

## TABLE OF CONTENTS

	<u>Page</u>
LIST OF FIGURES	ix
I. INTRODUCTION	1
II. THE REGENERATIVE LIQUID PROPELLANT GUN	1
III. BASIC ASSUMPTIONS	3
IV. GOVERNING EQUATIONS	4
A. LIQUID RESERVIOR	5
B. COMBUSTION CHAMBER	8
C. GUN TUBE	10
V. VENT OPTIONS	14
VI. PISTON RESISTANCE OPTIONS	15
A. PIS1	15
VII. PROJECTILE RESISTANCE OPTIONS	15
A. PROJ1	16
VIII. DISCHARGE COEFFICIENT - FROM RESERVOIR	16
A. DIS1	16
IX. DISCHARGE COEFFICIENT - FROM CHAMBER	16
X. MASS FLUX OPTIONS - FROM RESERVOIR	17
A. FLUX1	17
B. FLUX2	17
XI. MASS FLUX OPTIONS - FROM CHAMBER	18
A. FLUX1	18
XII. GUN TUBE PRESSURE DISTRIBUTION OPTIONS	18
A. TUBE1	18

XIII.	PRIMER OPTIONS	18
	A. PRIM1	19
	B. PRIM2	19
	C. PRIM3	19
XIV.	GUN TUBE HEAT LOSS OPTIONS	20
	A. HEAT1	20
	B. HEAT2	20
XV.	AIR SHOCK	21
	A. SHOCK1	21
	B. SHOCK2	21
XVI.	REPEAT OPTIONS	21
	A. REP1	22
	B. REP2	22
XVII.	CHAMBER PRESSURE OPTIONS	22
	A. CHAM1	22
	B. CHAM2	23
	C. CHAM3	23
XVIII.	DROPLET BURNING OPTIONS	23
	A. DROP1	29
	B. DROP2	29
	C. DROP3	29
	D. DROP4	30
XIX.	MASS AND ENERGY BALANCE	30
XX.	NUMERICAL METHOD	33
XXI.	GE 30MM GUN FIXTURE	33
	A. DESCRIPTION OF THE INPUT	36
	B. PRELIMINARY RUN	39
	C. MODELING - ROUNDS 4-10	43
	D. MODELING - ROUNDS 25-28	49
	E. DISCUSSION	55
XXII.	CONCLUSIONS	56
	REFERENCES	59

GLOSSARY	63
APPENDIX A	71
APPENDIX B	79
APPENDIX C	91
DISTRIBUTION LIST	97

## LIST OF FIGURES

<u>Figure</u>		<u>Page</u>
1	A Generic Reverse Annular Regenerative Liquid Propellant Gun.	2
2	GE 30mm Reverse Annular Regenerative Liquid Propellant Gun.	2
3	Experimental Chamber Pressure (line) and Liquid Pressure (dot) - Round 4.	34
4	Experimental Piston Travel - Round 4.	34
5	Actual Vent Area (line). Effective Area (dot). Round 4.	35
6	Experimental Chamber Pressure - Round 4 (line). Spline Fit to the Chamber Pressure (dot).	40
7	Experimental Piston Travel - Round 4 (line). Model with Experimental Chamber Pressure (dot).	40
8	Experimental Piston Travel - Round 4 (line). Computed Gun Recoil (dot).	41
9	Experimental Piston Travel - Round 4 (line). Model with Experimental Chamber Pressure. $C_D = 0.95$ (dot). $C_D = 0.85$ (dash). $C_D = 0.75$ (dot-dash).	42
10	Experimental Chamber Pressure - Round 4 (line). Model - Instantaneous Burning (dot).	44
11	Experimental Piston Travel - Round 4 (line). Model - Instantaneous Burning (dot).	44
12	Experimental Chamber Pressure - Round 4 (line). Model - Droplet Burning (dot).	45
13	Experimental Piston Travel - Round 4 (line). Model - Droplet Burning (dot).	45
14	Model - Droplet Diameter - Round 4.	46

15	Experimental Chamber Pressure - Round 4 (line). Mass in the Chamber/ Gun tube (dot). Liquid Accumulation (dash).	46
16	Experimental Chamber Pressure - Round 10.	48
17	Experimental Chamber Pressure (line) and Liquid Pressure (dot) - Round 25.	50
18	Experimental Piston Travel (line) and Computed Recoil (dot) - Round 25.	50
19	Experimental Chamber Pressure - Round 25 (line). Model - Droplet Burning (dot).	52
20	Experimental Piston Travel - Round 25 (line). Model - Droplet Burning (dot).	52
21	Model - Droplet Diameter - Round 25.	53
22	Experimental Chamber Pressure - Round 25 (line). Mass in the Chamber/ Gun Tube (dot). Liquid Accumulation (dash).	53
23	Experimental Chamber Pressure (line) and Liquid Pressure (dot) - Round 28.	54

## I. INTRODUCTION

In this paper a description of a reverse annular regenerative liquid propellant gun code is given. The basic governing equations for the lumped parameter model are similar to those developed for the in-line model,<sup>1-3</sup> and the derivations are not repeated in detail. Changes in the equations are described, and the reasons for the changes are given. A complete description of the present group of options is given. The code is compared to experimental data for a 30mm gun fixture developed by General Electric.<sup>4</sup> *Keywords: Gun; (KT)*

## II. THE REGENERATIVE LIQUID PROPELLANT GUN

Figure 1 shows a diagram of a generic regenerative liquid propellant gun with a reverse piston. The monopropellant in the liquid reservoir is around the gun tube. A primer is ignited and injects hot gas into the combustion chamber. As the chamber is pressurized, the piston is pushed to the right. Because of the piston area differential between the two regions, the piston will move forward even when the liquid pressure is higher than the intermediate chamber pressure. The pressure differential forces liquid propellant through the holes in the piston face and through the holes directly into the gun tube. The propellant ignites and burns in the chamber and in the tube. Hot gas may flow from the intermediate chamber into the tube or from the tube into the intermediate chamber, depending on the relative size of the injection areas. The increasing chamber pressure accelerates the piston, leading to more rapid injection. Eventually, the pressure pushes the projectile down the gun tube.

Figure 2 shows the design of the GE fixture. The booster at the left holds the igniter. Hot gas is vented from a series of holes around the booster. There are large slots in the stub case holder and the end of the short barrel, so the hot gas easily penetrates to the piston face. The piston face has no injection vents, which simplifies the propellant loading procedure. The liquid propellant is initially

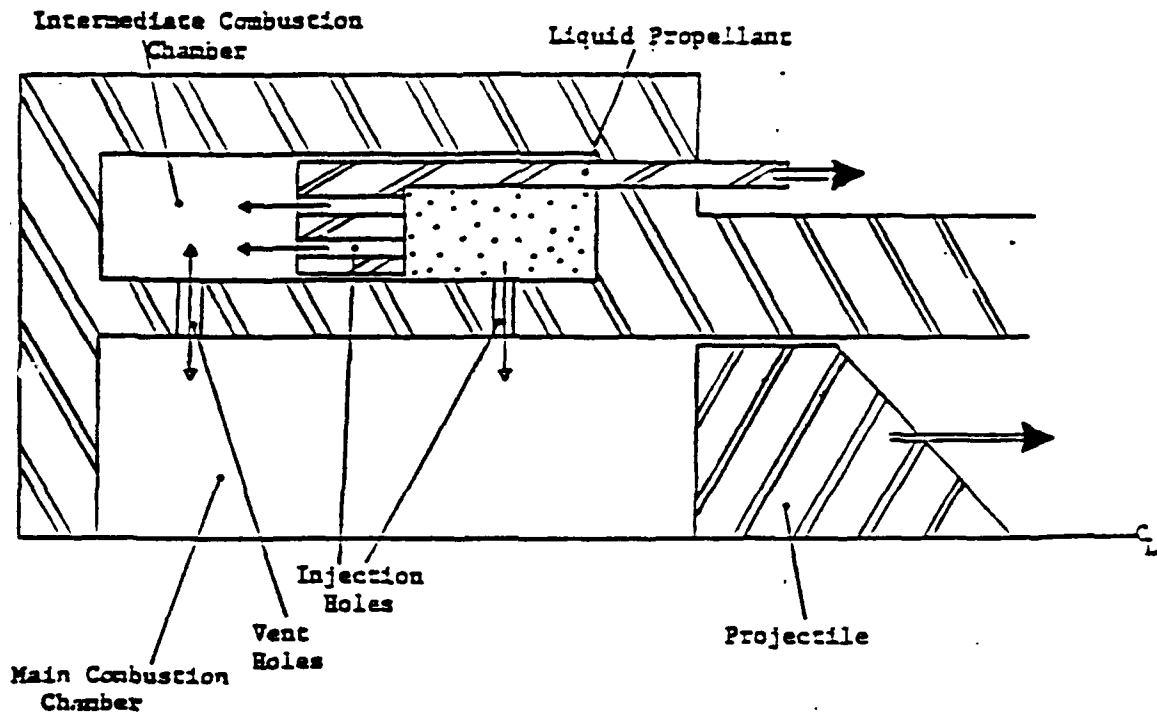


Figure 1. A Generic Reverse Annular Regenerative Liquid Propellant Gun.

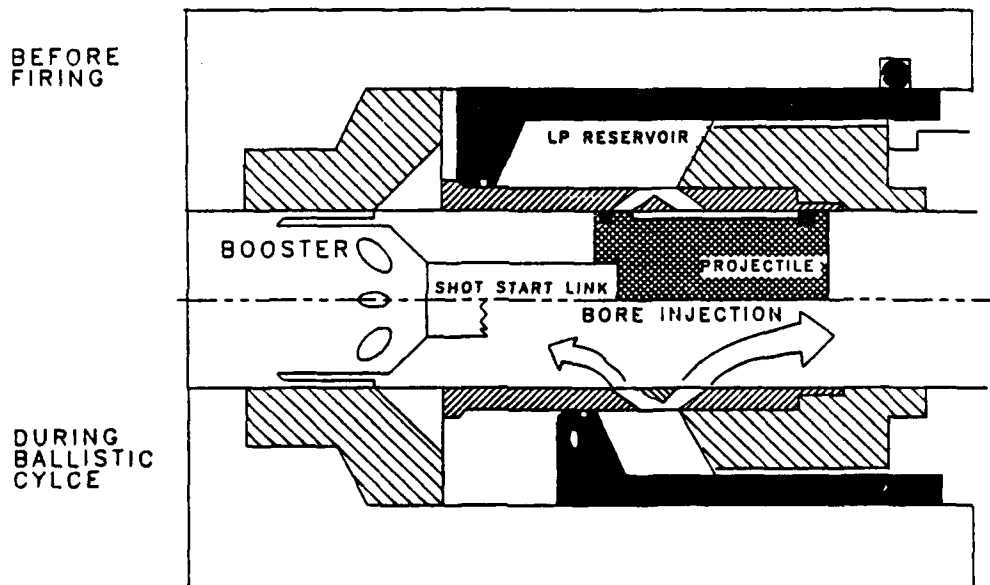


Figure 2. GE 30mm Reverse Annular Regenerative Liquid Propellant Gun.

around the short barrel between the piston and the valve head. The injection occurs through a series of "Y" shaped holes into the gun tube. The projectile initially blocks these holes. As the pressure increases, the tail seal at the end of the projectile flexes, allowing some liquid injection. At the desired shot start pressure, the shot start link breaks, releasing the projectile. The projectile then rapidly opens the injection holes, leading to rapid propellant injection. Near the end of the piston stroke, the piston partially blocks the injection ports. The liquid pressure rises, and brings the piston to a gradual stop.

### III. BASIC ASSUMPTIONS

The propellant in the liquid reservoir is assumed to be a homogeneous, isothermal fluid. Because of the high pressures in a gun, the liquid is considered to be compressible.

The piston and gun tube are assumed to be infinitely thin, that is, liquid moves instantaneously from the reservoir to the chamber/tube. The actual flow in the orifices is ignored. The mass flux out of the reservoir is normally computed assuming steady state Bernoulli flow. Comparisons with transient lumped parameter, one-dimensional, and two-dimensional models of the liquid reservoir indicate that this is a reasonable assumption.<sup>5</sup> As a first approximation, the liquid is assumed to combust instantaneously as soon as it enters the chamber or the gun tube, releasing all its energy. Later finite burning rate models for the liquid propellant will be introduced, in an attempt to model at least crudely the effects of propellant accumulation.

The intermediate chamber fluid is assumed to be homogeneous and stagnant. Lacking any detailed information on flow in the chamber, the fluid velocity in the chamber is simply set uniformly equal to zero.

The primer is assumed to have the same thermochemical properties as the propellant. The combustion and injection of the primer need not be

considered in detail. Instead the initial pressure in the chamber/tube is an input parameter. Then the amount of propellant needed to produce this pressure is calculated, and this is taken as the mass of the primer. The piston and projectile are not allowed to move during the burning of the primer. Later more complicated primer options will be discussed.

Unlike solid propellant guns, there is usually a large area change between the intermediate chamber and the gun tube. The mass flux into the gun tube is computed assuming steady state isentropic flow without loss terms.

The gun tube is also treated as a lumped parameter region, using the Lagrange pressure distribution that has successfully modeled the behavior of solid propellant guns<sup>6</sup>. The flow between the chamber and the tube is ignored, and the velocity at the end of the gun tube is set equal to zero. Because of the large area between the chamber and the tube, the flow velocities will be small here. The gun tube is treated as a simple cylinder, and the structure at the breech end of the gun is ignored. The projectile is also treated as a cylinder, and the tail seal is not modeled.

Below, we derive the governing equations for the simple lumped parameter model described here. Then a list of options will be given, with the appropriate modifications to the base governing equations.

#### IV. GOVERNING EQUATIONS

With the above assumptions, the regenerative gun behavior can be modeled by 13 ordinary differential equations. These equations are marked using numbers in square brackets at the left ([1] to [13]). Some algebraic equations are required to compute the coefficients of the ordinary differential equations. The equations describe the three lumped parameter regions (liquid reservoir, intermediate chamber, and

gun tube), the mass flux between the regions, and the piston and projectile motion. For historical reasons, the regions are numbered 1, 2, and 4. In a previous model<sup>3</sup> the back end of the gun tube was called the combustion chamber (region 3). Since this is just an extension of the gun tube, it is not considered a separate region in this report. Most of the derivations are the same as for the in line regenerative gun, and are not repeated in detail here. The notation is given in the glossary. For this section the chamber and the tube are assumed to contain only gas phase products.

#### A. LIQUID RESERVOIR

The equations governing the piston motion are straightforward. Let  $V_1$  be the volume of the propellant chamber, and  $A_1$  be the area of the propellant side of the piston (this area includes the vent holes). Let  $s_{ps}$  be the piston travel (to the right) and  $v_{ps}$  be the piston velocity. Then

$$[1] \quad \frac{dV_1}{dt} = -v_{ps} A_1 \quad (1)$$

The acceleration of the piston equals the force on the piston divided by the mass of the piston. That is,

$$[2] \quad \frac{dv_{ps}}{dt} = \frac{g_0}{M_{ps}} [p_2 (A_2 - A_g - A_{12}) - (p_1 + p_{ps}) (A_1 - A_{12})] \quad (2)$$

where  $A_2$  is the area of the combustion side of the piston,  $A_g$  is the area of the grease dyke between the piston and the chamber wall,  $A_{12}$  is the area of the hole in the piston,  $p_1$  is the pressure in the liquid chamber,  $p_2$  is the pressure in the combustion chamber, and  $M_{ps}$  is the mass of the piston. The quantity  $g_0 = 10^7$  gm/s-cm-MPa is a conversion constant to put the acceleration in the desired units of  $\text{cm}^2/\text{s}$ . By assumption, the pressures are constant throughout the two chambers. The

pressure in the grease dyke is normally very close to the chamber pressure, so it balances the chamber pressure on this part of the piston. The quantity  $p_{ps}$  is an empirical correction to simulate the effects of frictional resistance (see options). The piston is assumed initially to be prevented from moving toward the breech. So if the initial acceleration is negative, it is changed to zero. Also, the quantity  $p_{ps}$  is solely a resistance pressure. If the  $p_{ps}$  term is initially larger than the other pressure terms, the acceleration is set equal to zero. Also, if at a later time the piston reverses direction, the sign of  $p_{ps}$  is changed. The equation governing the piston travel is

$$[3] \quad \frac{ds_{ps}}{dt} = v_{ps} \quad (3)$$

From conservations of mass,

$$[4] \quad \frac{d\rho_1}{dt} = - \frac{\rho_1}{V_1} \frac{dV_1}{dt} - \frac{m_{12}}{V_1} - \frac{m_{14}}{V_1}, \quad (4)$$

where  $\rho_1$  is the density of the liquid,  $m_{12}$  is the mass flux from the reservoir into the chamber, and  $m_{14}$  is the mass flux from the reservoir into the gun tube. The energy equation can be expressed as

$$[5] \quad \frac{dp_1}{dt} = \frac{c_1^2}{g_0} \frac{d\rho_1}{dt}, \quad (5)$$

where  $c_1$  is the speed of sound in the liquid.

Heat transfer and temperature changes in the liquid propellant are expected to be small, and are ignored. Then the speed of sound is given by

$$c_1 = \sqrt{g_0 K / \rho_1}, \quad (6)$$

where  $K$  is the adiabatic bulk modulus. For the common liquid propellants, this can be fit very accurately by<sup>7</sup>

$$K = K_1 + K_2 P_1 \quad (7)$$

The corresponding equation of state is

$$P_1 = \frac{K_1}{K_2} [(\rho_1/\rho_0)^{K_2} - 1] \quad (8)$$

The ordinary differential equation [5] for the pressure is not actually required. Once the density is known, the pressure can be computed from the equation of state (8).

Recently an equation of state has been derived that also includes the temperature dependence.<sup>8</sup> This could be used instead to include temperature changes in the liquid. The new equation predicts almost the same pressure dependence as eq. (8).

The mass flux from the reservoir into the chamber is assumed to be steady state Bernoulli flow

$$m_{12} = C_D A_{12} \sqrt{2g_0 \rho_1 (P_1 - P_2)} \quad (9)$$

The discharge coefficient  $C_D$  is an empirical correction to the equations to take into account frictional losses. Since the mass flux for a gun firing is not steady state,  $C_D$  may also be used to approximate the time delay in reaching steady state.

Similarly, the mass flux from the reservoir into the gun tube is given by

$$m_{14} = C_D A_{14} \sqrt{2g_0 \rho_1 (P_1 - P_h)} \quad (10)$$

where  $p_h$  is the pressure in the gun tube at the injection holes (see Section C below). The same discharge coefficient is used for both injection processes.

The vent area  $A_{14}$  must be calculated. A "Y" shaped vent is assumed (see Figure 2). The vent openings are considered to be circular. First the position of the piston is calculated. If the piston has reached the injection holes, it partially blocks the holes. The area not blocked by the piston is calculated. A similar procedure is carried out on the gun tube side. The initial position of the projectile is used to calculate how much of the piston side holes are blocked. The vent area between the reservoir and the tube is taken to be the smaller of these two areas. If a simple cylindrical vent is used instead of a "Y" vent, the area of the second set of holes in the gun tube is set equal to zero.

#### B. COMBUSTION CHAMBER

Now consider the combustion chamber. By analogy with eq. [1],

$$[6] \quad \frac{dV_2}{dt} = v_{ps} A_2, \quad (11)$$

where  $V_2$  is the volume of the combustion chamber and  $A_2$  is the area of the combustion side of the piston (including holes). Similarly, from conservation of mass

$$[7] \quad \frac{d\rho_2}{dt} = -\frac{\rho_2}{V_2} \frac{dV_2}{dt} + \frac{m_{12} - m_{24}}{V_2}, \quad (12)$$

where  $\rho_2$  is the density of the gas in the combustion chamber and  $m_{24}$  is the mass flux into the gun tube. The energy equation is

$$\begin{aligned}
 [8] \quad \frac{dp_2}{dt} = & \frac{c_2^2}{g_0} \frac{d\rho_2}{dt} + \frac{m_{12} (h_{L1} - h_{G2}) (\gamma - 1)}{V_2 - b M_2} \\
 & - \frac{m_{24} (h_{G4} - h_{G2}) (\gamma - 1)}{V_2 - b M_2} ,
 \end{aligned} \tag{13}$$

where  $c_2$  is the speed of sound in the chamber,  $h_{L1}$  is the enthalpy of the liquid,  $h_{G2}$  is the enthalpy of the chamber gas,  $h_{G4}$  is the enthalpy of the gun tube gas, and  $m_{24}$  is the mass flux from the chamber into the tube. The last term only appears if  $m_{24}$  is negative, since flux out of the region will not effect the enthalpy. The energy equation is based on the Noble-Abel equation of state<sup>6</sup>

$$p_2 = \rho_2 R_s T_2 / (1 - b \rho_2) , \tag{14}$$

where  $T_2$  is the temperature in region 2,  $R_s$  is the specific gas constant (universal gas constant divided by molecular weight of the gas), and  $b$  is the covolume. This can also be written as

$$p_2 = \rho_2 (\gamma - 1) c_v T_2 / (1 - b \rho_2) , \tag{15}$$

where  $c_v$  is the specific heat at constant volume and  $\gamma$  is the specific heat ratio  $c_p/c_v$ . The corresponding equation for the speed of sound is

$$c_2 = \sqrt{\frac{g_0 \gamma p_2}{\rho_2 (1 - b \rho_2)}} . \tag{16}$$

The energy content of a propellant is normally given in terms of impetus  $\lambda$ . Consider a quantity of propellant in a constant volume closed chamber. The propellant combusts, and the result is a gas with some molecular weight  $M_g$  and temperature  $T_0$  (called the isochoric temperature). The impetus is defined as

$$\lambda = R_u T_0 / M_g , \tag{17}$$

where  $R_u$  is the universal gas constant. Impetus can be obtained from a closed bomb experiment, if the proper corrections are made for the primer and the heat loss to the chamber walls. For liquid propellants, the impetus has been calculated by a thermodynamics code.<sup>9</sup> The values of the molecular weight, the specific heats, and the covolume of the product gases are evaluated at the isochoric temperature and then assumed to be constant with respect to temperature and pressure. The impetus does depend on the initial loading density (grams of propellant per unit volume). Values are chosen at a nominal loading density of 0.2 g/cc. If the values are instead chosen for some other loading density, the effects are negligible.

For our case, it is more convenient to work with the chemical energy

$$e_1 = \lambda / (\gamma - 1) . \quad (18)$$

The enthalpy of the liquid is given by

$$h_{L1} = e_1 + P_1 / \rho_1 . \quad (19)$$

The enthalpy of the gas is given by

$$h_{G2} = c_v T_2 + P_2 / \rho_2 = c_p T_2 + b P_2 . \quad (20)$$

### C. GUN TUBE

Finally, the gun tube (region 4) is considered to be a simple cylinder. The structure shown in Figure 2 is ignored. The volume has the standard equation

$$[9] \quad \frac{dV_4}{dt} = v_{pj} A_4, \quad (21)$$

where  $v_{pj}$  is the velocity of the projectile and  $A_4$  is the area of the gun tube. The rapid projectile motion creates a large pressure gradient. The standard approach is to use a Lagrange pressure distribution,<sup>6</sup> that is, assume that the density is constant with respect to space. It follows from the one-dimensional continuity equation that the gas velocity is a linear function of distance. The gas velocity at the base of the projectile is equal to the velocity of the projectile. In solid propellant guns, the gas velocity at the other end of the gun (breech) is assumed to be zero. Since there is a mass flow into the gun tube, this is not correct for our model. However, present designs have a large area between the chamber and the tube, and the corresponding velocity is relatively small. In this case the standard Lagrange approximation is accurate.

Integrating the momentum equation,

$$p(x) = p_L - (p_R - p_{pj}) \frac{M_4}{2M_{pj}} \frac{x^2}{x_R^2}, \quad (22)$$

where  $x_R$  is the distance from the back end of the tube to the base of the projectile,  $p_L$  is the pressure at the back of the gun tube,  $p_R$  is the pressure at the base of the projectile,  $M_4$  is the mass of the gas in the tube,  $M_{pj}$  is the mass of the projectile, and  $p_{pj}$  is the resistance pressure. The latter is an input parameter, which takes into account the shot start engraving force and the frictional forces between the projectile and the bore. Evaluating at  $x=x_R$  yields

$$p_R = p_L - \frac{M_4}{2M_{pj}} (p_R - p_{pj}). \quad (23)$$

Integrating equation (21) from the breech to the projectile base yields

$$p_4 = p_L - \frac{M_4}{6M_{pj}} (p_R - p_{pj}) , \quad (24)$$

where  $p_4$  is the space mean pressure. Then the above two equations can be solved for  $p_L$  and  $p_R$ . Equation (22) can be used to compute  $p_h$ , which is taken to be the pressure at the center of the first set of gun tube holes.

The above two equations assume that the projectile has started to move, creating a pressure differential. If the projectile has not moved, then region 4 is treated as a stagnant homogenous region like region 2, and the pressure is uniform.

Given the pressure on the projectile, the acceleration equation is

$$[10] \quad \frac{dv_{pj}}{dt} = (p_R - p_{pj}) A_4 g_0 / M_{pj} . \quad (25)$$

As with the piston, the pressure  $p_{pj}$  is only a resistive pressure. If  $p_{pj} > p_R$ , the projectile does not move. The projectile travel  $s_{pj}$  is given by

$$[11] \quad \frac{ds_{pj}}{dt} = v_{pj} . \quad (26)$$

The last two differential equations are exactly analogous to region 2. That is,

$$[12] \quad \frac{d\rho_4}{dt} = - \frac{\rho_4}{V_4} \frac{dV_4}{dt} + \frac{m_{14}}{V_4} + \frac{m_{24}}{V_4} , \quad (27)$$

where  $\rho_4$  is the space mean average density of the gas in region 4, and

$$\begin{aligned}
 [13] \quad \frac{dp_4}{dt} = & \frac{c_4^2}{g_0} \frac{d\rho_4}{dt} + \frac{m_{14} (h_{L1} - h_{G4}) (\gamma - 1)}{V_4 - b M_4} \quad (28) \\
 & + \frac{m_{24} (h_{G2} - h_{G4}) (\gamma - 1)}{V_4 - b M_4} .
 \end{aligned}$$

The last term only appears if  $m_{24}$  is positive ( $p_2 > p_L$ ). The average speed of sound in the tube is

$$c_4 = \sqrt{\frac{g_0 \gamma p_4}{\rho_4 (1 - b \rho_4)}} . \quad (29)$$

The mass flux from the chamber into the gun tube is assumed to be isentropic flow (that is, adiabatic and reversible).<sup>10,11</sup> Assume that  $p_2$  is greater than  $p_L$ . Then  $m_{24}$  is positive. The gas in the chamber is considered to be stagnant, and expands isentropically into the gun tube. The expanded gas then mixes with the gun tube gas already present. The process equations for a Noble-Abel equation of state are

$$T (1/\rho - b)^{(\gamma-1)} = \text{constant} , \quad (30)$$

and

$$p (1/\rho - b)^\gamma = \text{constant} . \quad (31)$$

Assume that  $p_t = p_L$ , since the pressure will equilibrate much more rapidly than the temperature or density. The process equations (30) and (31) can be used to find the throat temperature  $T_t$  and density  $\rho_t$ . Then the one-dimensional momentum equation can be integrated from the stagnant conditions in the chamber to the throat, resulting in

$$v_t = \sqrt{2g_0 (b(p_2 - p_t) + c_p T_t [(p_2/p_t)^{(\gamma-1)/\gamma} - 1])} \quad (32)$$

and

$$\dot{m}_{24} = C_D' A_{24} \rho_t v_t , \quad (33)$$

where  $A_{24}$  is the area between the chamber and the tube. The discharge coefficient  $C_D'$  is as before an empirical correction for loss terms. Due to lack of better information, this is set to one.

If the flow is from the tube into the chamber, then  $p_t = p_2$ . The process equations (30) and (31) are again used to find the throat temperature  $T_t$  and density  $\rho_t$ . The flow is described by

$$v_t = \sqrt{2g_0 (b(p_L - p_t) + c_p T_t [(p_L/p_t)^{(\gamma-1)/\gamma} - 1])} \quad (34)$$

and

$$\dot{m}_{24} = -C_D' A_{24} \rho_t v_t . \quad (35)$$

#### V. VENT OPTIONS

Unlike the in-line regenerative gun code, there is a standard setup for the vents. The vent area  $A_{12}$  between the reservoir and the chamber is constant.

The vents into the gun tube are "Y" shaped. On the reservoir side, there is a single set of circular holes. The area of each hole and the number of holes is read in, as well as the distance the piston must travel to reach the center of the holes. As the piston moves, a check is made to see if the piston partially blocks the holes. If so, the area covered by the piston is computed. On the gun tube side, there are two sets of holes. The gun tube is treated as a simple cylinder. The area of each set of holes is read in, as well as the distance from the end of the gun tube to the center of the holes. The number of holes is assumed to match the number of holes on the reservoir side. The projectile is also treated as a simple cylinder. The initial

offset of the projectile from the end of the tube is entered. From the position of the holes and the projectile, the area blocked by the projectile is computed. The actual vent area  $A_{14}$  is taken to be the minimum of the reservoir and tube areas. There is no attempt to model the tail seal.

In practice, since the holes in the short barrel are drilled on a slant, the openings will be elliptical rather than circular. Using circular openings in the code results in only minor errors in the vent area.

## VI. PISTON RESISTANCE OPTIONS

As the piston moves, there is frictional resistance between the piston and the chamber walls. There is no good estimate for the size of this frictional resistance. Because of the large pressures involved and the relatively slow speed of the piston, this effect is not expected to be important. Nevertheless, piston resistance options are included. Only one option is presently in the code.

### A. PIS1

The resistance is considered to be solely a function of piston travel. A table of piston travel versus resistive pressures is read in. The table will be normalized to the maximum piston travel. The piston resistive pressure  $p_{ps}$  at any given piston travel  $s_{ps}$  is found by interpolation. The actual resistive force is  $p_{ps} (A_1 - A_{12})$ . An equivalent pressure is read in rather than the actual force to make it easier to compare the braking force exerted by friction with the braking force exerted by the liquid.

## VII. PROJECTILE RESISTANCE OPTIONS

Similarly, as the projectile moves, there is friction between the

projectile and the gun tube. More important is the shot start pressure. The projectile is restrained from moving until the pressure at its base reaches an appropriate value. The choice of shot start pressure can have a large effect on performance and on the maximum pressures in the gun. At present there is only one option.

#### A. PROJ1

As with the piston, a table of projectile travel versus resistive pressure is read in. The table is not normalized. The resistive pressure  $p_{pj}$  for any given projectile travel  $s_{pj}$  is found by interpolation. If  $s_{pj}$  is larger than the last table entry for travel, the last table entry for pressure is chosen. The actual resistive force is  $p_{pj} A_4$ . The first entry in the table is the shot start pressure. The projectile will not move until the tube pressure reaches the shot start pressure.

### VIII. DISCHARGE COEFFICIENT - FROM RESERVOIR

The discharge coefficients needed in equations (9) and (10) are input parameters. The same discharge coefficient is used for both injection processes out of the reservoir.

#### A. DIS1

A table of piston travel versus discharge coefficient is read in. The table is normalized to the maximum piston travel. The discharge coefficient  $C_D$  for any given piston travel  $s_{ps}$  is found by interpolation.

### IX. DISCHARGE COEFFICIENT - FROM CHAMBER

The discharge coefficient needed in equations (33) and (35) is assumed to be one. There is normally a large area between the

intermediate chamber and the gun tube, and loss terms are expected to be very small.

## X. MASS FLUX OPTIONS - FROM RESERVOIR

### A. FLUX1

Steady state Bernoulli flow is assumed. The mass flux  $m_{12}$  is computed using equation (9), and  $m_{14}$  is computed using equation (10). The routine computes the Weber number, the Reynold's number, and the third Lagrange number for  $m_{14}$ , which is the primary injection flow. While this code does not use these numbers, they are printed out as additional information about the injection process.

### B. FLUX2

Since the gun environment is highly transient, steady state flow may not be a good approximation. A transient model for injection has been developed.<sup>5,12</sup> At the present this is only implemented for flow  $m_{14}$ . For this option the vent area in the piston  $A_{12}$  must be set to zero (no injection through the piston face). The basic assumption is that the space derivative of the mass flux  $\rho vA$  of the fluid in the reservoir is zero. Then the one-dimensional momentum equations can be integrated from the piston to the vent with the result

$$[F1] \quad \frac{d(\rho vA)}{dt} = [0.5\rho_1(v_{ps}^2 - v_{14}^2) + g_0 C_D^2 (p_1 - p_h)] / \int dx/A \quad (36)$$

where  $v_{14}$  is the velocity of the fluid entering the tube. This additional ordinary differential equation is integrated to obtain the mass flux rate into the chamber. The equation shows a rapid rise to values near steady state.

## XI. MASS FLUX OPTIONS - FROM CHAMBER

### A. FLUX1.

Steady state isentropic flow is assumed. The mass flux into the gun tube is computed using eq. (33) or (35).

## XII. GUN TUBE PRESSURE DISTRIBUTION OPTIONS

Recently a number of different assumptions for the gun tube pressure distribution were implemented and tested against a one-dimensional code.<sup>13</sup> However, for the present case the standard Lagrange distribution is reasonable.

### A. TUBE1

The standard Lagrange pressure distribution is assumed, that is, the density is constant in the tube, which implies that the velocity is linear. For the purpose of computing the pressure distribution, the velocity at the back end of the gun tube is set equal to zero. The momentum equation is integrated to obtain a formula for the pressure  $p(x)$  in the tube. The pressure  $p_R$  at the base of the projectile and the pressure  $p_L$  at the back end of the gun tube are computed using eq. (23) and (24). The injection into the gun tube will effect the pressure distribution. However, the injection velocities are small compared to the projectile velocity. Since the injection is radial, there is no obvious way to modify the Lagrange distribution to take the injection into account.

## XIII. PRIMER OPTIONS

In present liquid propellant guns, a solid primer is used. The primer is in the booster cavity. The primer injects hot gas through large holes into the gun tube/chamber to begin the firing cycle. The

exact details of the primer model have only a small effect on pressure, so simplifications have been made. First, the primer is assumed to be the same material as the liquid propellant, so a new set of properties for the actual solid primer does not have to be read in. Three primer options then offer varying levels of simplification.

#### A. PRIM1

It is assumed that the primer completely combusts before the start of the calculation, pressurizing the chamber. The corresponding piston movement is ignored. The code computes how much propellant would be necessary to create the input chamber pressure, and records this as the primer weight.

#### B. PRIM2

The initial mass of the primer is read in. Then the primer is distributed evenly in the chamber and tube as liquid droplets. A droplet burning option must be chosen (see below). The size of the droplets is determined from the drop diameter in the droplet burning option. This option can be used to mimic the delay in time to reach the primer pressure.

#### C. PRIM3

The primer is out of the system. The mass of the primer, the injection time, and a heat loss term are read in. The primer is then injected at a steady rate into the gun tube over the desired time interval. The primer is assumed to combust instantaneously as it enters the tube. Since primer gases are often injected through long narrow tubes, heat loss is important. To take heat loss into account, the chemical energy of the propellant is multiplied by the heat loss factor. During the injection process, the gun tube density and pressure equations are modified

$$[12] \quad \frac{d\rho_4}{dt} = \dots + \frac{\dot{m}_{p4}}{V_4}, \quad (37)$$

$$[13] \quad \frac{dp_4}{dt} = \dots + \frac{\dot{m}_{p4} (e_1 * l_p - h_{G4}) (\gamma - 1)}{V_4 - b M_4}, \quad (38)$$

where  $\dot{m}_{p4}$  is the mass flux of primer into the tube and  $l_p$  is the heat loss term.

#### XIV. GUN TUBE HEAT LOSS OPTIONS

In gun systems there is a large energy flux from the hot gas to the gun tube. This is important for actual systems primarily because it causes erosion of the gun tube. The effect on muzzle velocity and pressure is on the order of a few percent. Heat loss is often treated as an adjustable parameter for fine tuning a model to agree with experiment.

##### A. HEAT1

The heat loss to the gun tube walls is ignored. This causes a slight increase in muzzle velocity and maximum pressures.

##### B. HEAT2

There is heat loss to the gun tube. A correlation developed for turbulent pipe flow is used.<sup>2</sup> An assumed gun tube temperature  $T_w$  is read in and assumed to remain constant. The equation for the space mean pressure is modified by

$$[13] \quad \frac{dp_4}{dt} = \dots - \frac{Q_w (\gamma - 1)}{(1 - b \rho_4)} \quad (39)$$

where  $Q_w$  is the heat loss to the tube wall. Simulations run so far with the code indicate a heat loss of 3% to 5% for 120mm guns, and 10% to 12% for 30mm guns. These numbers are in the range reported by Nordheim, Soodak, and Nordheim<sup>14</sup> for their analysis of experimental data, and comparable with the heat loss normally used in solid propellant gun modeling. If desired, the heat loss can be adjusted up or down.

#### XV. AIR SHOCK

The projectile will compress the air in the tube as it accelerates. This will have a minor effect on the velocity of the projectile.

##### A. SHOCK1

The resistance due to the air shock in front of the projectile is ignored.

##### B. SHOCK2

The resistance pressure  $p_s$  is calculated using a formula developed by Corner<sup>6</sup> for the air shock based on the Rankine-Hugoniot relations. This new resistance pressure  $p_s$  is just added on to the frictional resistance pressure  $p_{pj}$ .

#### XVI. REPEAT OPTIONS

In systems studies, there is often a physical constraint on the class of acceptable solutions. One common constraint is implemented in the code. The code will integrate repeatedly until the constraint is satisfied.

A. REP1

The code integrates once. This is the standard option.

B. REP2

A solution is sought with a given maximum liquid pressure. The liquid pressure is adjusted by changing the vent area into the gun tube on the liquid side. The desired liquid pressure and a first guess for the vent increment is read in.

The problem is first integrated with the input conditions. If the maximum liquid pressure is too low, the vent area is incremented by the input value. If the liquid pressure is too low, the vent area is decremented. Once values are obtained both above and below the desired maximum liquid pressure, interpolation is used to obtain the new vent area. Convergence normally occurs after a small number of integrations.

## XVII. CHAMBER PRESSURE OPTIONS

It is convenient to isolate part of the model for study. For instance, suppose that the model chamber pressure is slightly high. This raises the piston acceleration and increases the rate of injection of the propellant. As the propellant burns, the chamber pressure rises. After a short time, the model chamber pressure and piston travel are substantially too large. So to study the liquid injection process, it is better to disconnect the chamber pressure from the injection.

A. CHAM1

The chamber pressure is computed using the usual equations.

## B. CHAM2

The experimental chamber pressure versus time is read in. At each time step, an interpolated experimental chamber pressure overwrites the pressure computed using the ordinary differential equation [8]. This allows a study of the injection process and the projectile motion using the experimental data as a boundary condition.

## C. CHAM3

The time derivative of the experimental chamber pressure is read in. This is normally found by making a spline fit of the chamber pressure and taking the derivative of the spline. At each time step, an interpolated derivative overwrites the derivative computed from the ordinary differential equation [8]. This is more stable than the CHAM2 option, and larger time steps will be taken. The code runs substantially faster, although the same answer will be obtained.

## XVIII. DROPLET BURNING OPTIONS

So far the liquid has been assumed to combust instantaneously upon exiting the reservoir. However, liquid accumulation in the gun tube is very important for some cases. So simple rules are derived for the formation and combustion of droplets in the gun tube/chamber. In the model, the liquid is assumed to instantaneously form droplets of fixed size as the liquid enters the gun tube. The droplets are evenly distributed in the tube. Flow into the intermediate chamber will include droplets. The droplets will then combust at some given rate. The initial size of the droplets is an input parameter. This simplified model allows the code to determine the effects of liquid accumulation.

The derivation of the relevant equations is very similar to the previous reports. Let  $M_{L2}$  be the liquid mass in region 2,  $V_{L2}$  be the liquid volume,  $M_{G2}$  be the gas mass, and  $V_{G2}$  be the gas volume. Then

$$\rho_{L2} = \frac{M_{L2}}{V_{L2}}, \quad (40)$$

and

$$\rho_{G2} = \frac{M_{G2}}{V_{L2}}, \quad (41)$$

where  $\rho_{L2}$  is the density of the liquid and  $\rho_{G2}$  is the density of the gas. Define the porosity

$$\epsilon_2 = \frac{V_{G2}}{V_2}. \quad (42)$$

Then

$$\rho_2 = \frac{M_2}{V_2} = (1 - \epsilon_2) \rho_{L2} + \epsilon_2 \rho_{G2}. \quad (43)$$

Following eq. (6), the speed of sound in the liquid is

$$c_{L2} = \sqrt{g_0 K / \rho_{L2}}, \quad (44)$$

and following eq. (16) the speed of sound in the gas is

$$c_{G2} = \sqrt{\frac{g_0 \gamma P_2}{\rho_{G2} (1 - b \rho_{G2})}}. \quad (45)$$

Assuming the gas and liquid pressure are the same, the speed of sound  $c_2$  in the mixture is given by

$$c_2 = \sqrt{\frac{1}{\rho_2} \left[ \frac{1}{\epsilon_2 / (\rho_{G2} c_{G2}^2) + (1 - \epsilon_2) / (\rho_{L2} c_{L2}^2)} \right]} \quad (46)$$

The enthalpy of the liquid is

$$h_{L2} = e_1 + P_2 / \rho_{L2} \quad (47)$$

where  $e_1$  is the chemical energy of the liquid, and the enthalpy of the gas is

$$h_{G2} = c_p T_2 + b P_2 \quad (48)$$

The thirteen equations derived in Section IV remain the same except for the energy equations [8] and [13]. The energy equation is written in the more general form

$$[8] \quad \frac{dp_2}{dt} = \frac{\rho_2 c_2^2}{g_0 V_2} \left( - \frac{dV_2}{dt} + \frac{m_{L2}}{\rho_{L2}} + \frac{m_{G2}}{\rho_{G2}} + \frac{S_2 g_0 (\gamma - 1)}{\rho_{G2} c_{G2}^2 (1 - b \rho_{G2})} \right) \quad (49)$$

Here  $m_{L2}$  is the rate of production of liquid in the chamber. In this case,

$$m_{L2} = m_{12} - m_2 - m_{24} \frac{M_{L2}}{M_2}, \quad m_{24} > 0 \quad (50)$$

$$m_{L2} = m_{12} - m_2 - m_{24} \frac{M_{L4}}{M_4}, \quad m_{24} < 0 \quad (51)$$

with  $m_2$  the rate at which combustion is turning the liquid into gas. The rate depends on whether fluid is flowing from the chamber to the

tube ( $m_{24} > 0$ ) or from the tube into the chamber ( $m_{24} < 0$ ). The rate of production of gas  $m_{G2}$  is given by

$$m_{G2} = m_2 - m_{24} \frac{M_{G2}}{M_2}, \quad m_{24} > 0 \quad (52)$$

$$m_{G2} = m_2 - m_{24} \frac{M_{G4}}{M_4}, \quad m_{24} < 0 \quad (53)$$

The rate of production of mass times the change in enthalpy  $S_2$  is given by

$$S_2 = m_2 (h_{L2} - h_{G2}) + m_{12} (h_{L1} - h_{L2}), \quad m_{24} > 0 \quad (54)$$

$$S_2 = m_2 (h_{L2} - h_{G2}) + m_{12} (h_{L1} - h_{L2}) \quad m_{24} < 0 \quad (55)$$

$$- m_{24} (h_{G4} - h_{G2}) \frac{M_{G4}}{M_4} - m_{24} (h_{L4} - h_{L2}) \frac{M_{L4}}{M_4}.$$

In the gun tube, the equations are exactly analogous. The only difference is in the coefficients for the pressure equation

$$[13] \quad \frac{dp_4}{dt} = \frac{\rho_4 c_4^2}{g_0 V_4} \left( - \frac{dV_4}{dt} + \frac{m_{L4}}{\rho_{L4}} + \frac{m_{G4}}{\rho_{G4}} + \right. \quad (56)$$

$$\left. \frac{S_4 g_0 (\gamma - 1)}{\rho_{G4} c_{G4}^2 (1 - b \rho_{G4})} \right).$$

In the gun tube

$$m_{L4} = m_{14} - m_4 + m_{24} \frac{M_{L2}}{M_2}, \quad m_{24} > 0 \quad (57)$$

$$m_{L4} - m_{14} = m_4 + m_{24} \frac{M_{L4}}{M_4}, \quad m_{24} < 0 \quad (58)$$

$$m_{G4} = m_4 + m_{24} \frac{M_{G2}}{M_2} + m_{p4}, \quad m_{24} > 0 \quad (59)$$

$$m_{G4} = m_4 + m_{24} \frac{M_{G4}}{M_4} + m_{p4}, \quad m_{24} < 0 \quad (60)$$

$$S_4 = m_4 (h_{L4} - h_{G4}) + m_{14} (h_{L1} - h_{L4}) \quad m_{24} > 0 \quad (61)$$

$$+ m_{24} (h_{G2} - h_{G4}) \frac{M_{G2}}{M_2} + m_{24} (h_{L2} - h_{L4}) \frac{M_{L2}}{M_2}$$

$$+ m_{p4} (e_1 - h_{G4}),$$

$$S_4 = m_4 (h_{L4} - h_{G4}) + m_{14} (h_{L1} - h_{L4}) \quad m_{24} < 0 \quad (62)$$

$$+ m_{p4} (e_1 - h_{G4}),$$

If there is heat loss in the gun tube, the modification term from eq. (39) is included.

To complete the system, ordinary differential equations are required to determine the liquid density and mass. The corresponding gas quantities can then be easily derived. The basic assumption is that the pressure in the liquid and the gas in a given region is the same. Since the gas pressure is known, the liquid equation of state can be written in differential form as

$$[14] \quad \frac{d\rho_{L2}}{dt} = \frac{g_0}{c_{L2}^2} \frac{dp_2}{dt}, \quad (63)$$

and

$$[16] \quad \frac{d\rho_{L4}}{dt} = \frac{g_0}{c_{L4}^2} \frac{dp_4}{dt} \quad (64)$$

The mass conservation equations for the liquid have already been derived

$$[15] \quad \frac{dM_{L2}}{dt} = m_{L2} \quad (65)$$

and

$$[17] \quad \frac{dM_{L4}}{dt} = m_{L4} \quad (66)$$

To close the system, the rate at which the liquid droplets are combusting must be known. The rate of surface regression is assumed to be of the form

$$\text{rate of surface regression} = Ap^B \quad (67)$$

Liquid propellant burning rates have been measured by McBratney<sup>15,16</sup>. The rate of combustion is

$$m_2 = \rho_{L2} S Ap^B \quad (68)$$

where  $S$  is the total surface area of the droplets in a region. All the droplets are assumed to have a constant diameter  $d$ . So the total surface area in the region

$$S = 6 V_{L2} / d \quad (69)$$

and eq. (68) can be written as

$$m_2 = M_{L2} (6/d) A p_2^B . \quad (70)$$

For region 4, the pressure is no longer constant over the region, but follows the Lagrange pressure distribution. This would be quite complicated to keep track of, so the combustion rate is assumed to depend on the average pressure  $p_4$ , and

$$m_4 = M_{L4} (6/d) A p_4^B . \quad (71)$$

The droplet options can now be described.

#### A. DROP1

The liquid is assumed to combust instantaneously as soon as it enters the gun tube/chamber. This is the model described in section IV.

#### B. DROP2

The liquid exits the reservoir and instantaneously forms droplets of diameter  $d$ . The size of the droplets is fixed in time and space. As the droplets burn, the number of droplets may decrease, but the size of the droplets remains unchanged.

The droplet diameter and the burning rate coefficients are read in. There is some evidence that the burning rate for liquid monopropellants has a sharp slope break around 100 MPa. So the burning rate is read in as two functions, and the pressure is specified at which the change is made from the low pressure rate to the high pressure rate.

#### C. DROP3

The droplet size is fixed in space, but not in time. A table of droplet diameters versus piston travel is read in. As usual, the table

is scaled to the maximum piston travel.

While this model is unrealistic, it allows the modeling of various accumulation rates at different times in the firing cycle.

#### D. DROP4

This is like the option DROP3, except the table of droplet diameters is read in versus the projectile travel.

### XIX. MASS AND ENERGY BALANCE

As a check on the equations derived, both mass and energy should be conserved. The mass balance is straightforward.

$$M_T = M_1 + M_{L2} + M_{G2} + M_{L4} + M_{G4} + M_p \quad (72)$$

where  $M_p$  is the mass of the primer and  $M_T$  is the total mass of the propellant and primer.  $M_T$  should be constant throughout the integration.

The energy balance is more complicated. The liquid is considered to be an isothermal fluid, and its internal energy  $e_1$  is just the chemical energy of the propellant. The total energy in region 1 is

$$E_1 = e_1 M_1 \quad (73)$$

If the outside primer option is chosen (PRIM3) then

$$E_p = e_1 M_p \quad (74)$$

The internal energy of the liquid in region 2 is given by

$$E_{L2} = e_1 M_{L2} , \quad (75)$$

and the internal gas energy is

$$E_{G2} = c_v T_2 M_{G2} . \quad (76)$$

Similarly for region 4

$$E_{L4} = e_1 M_{L4} , \quad (77)$$

and

$$E_{G4} = c_v T_4 M_{G4} . \quad (78)$$

The kinetic energy of the piston is given by

$$EK_{ps} = 0.5 M_{ps} v_{ps}^2 / g_0 , \quad (79)$$

and the kinetic energy of the projectile by

$$EK_{pj} = 0.5 M_{pj} v_{pj}^2 / g_0 . \quad (80)$$

The liquid and gas in region 4 are moving, and are assumed to have the same velocity. The kinetic energy of the liquid is

$$EK_{L4} = 0.5 M_{L4} v_{pj}^2 x_R / (3g_0) , \quad (81)$$

where  $x_R$  is the distance from the back of the gun tube to the base of the projectile. The kinetic energy of the gas is

$$EK_{G4} = 0.5 M_{G4} v_{pj}^2 x_R / (3g_0) . \quad (82)$$

The fluid in the chamber is considered stagnant. When the fluid

enters the gun tube, it instantaneously acquires kinetic energy. To keep the energy balanced, the enthalpy of the liquid in the gun tube is redefined as

$$h_{L4} = e_1 + p_4 / \rho_{L4} + EK_{L4} / M_4 , \quad (83)$$

and the enthalpy of the gas in the gun tube is

$$h_{G4} = c_p T_4 + b p_4 + EK_{G4} / M_4 . \quad (84)$$

The heat loss to the gun tube is energy that leaves the system. The total energy loss is approximated by finite differences. The code is set up to print out information at designated time intervals. After each time interval, the heat loss from the gun tube is approximated by

$$EH_4(t) = EH_4(t_0) + Q_w V_4 (t-t_0) , \quad (85)$$

where  $Q_w$  and  $V_4$  are averages of the values at the present time  $t$  and the old time  $t_0$ .

The energy lost through friction is approximated in a similar fashion. The energy lost is equal to force times distance, or

$$EF_{ps}(t) = EF_{ps}(t_0) + p_{ps} (A_1 - A_{12})(s_{ps}(t) - s_{ps}(t_0)) \quad (86)$$

for the piston and

$$EF_{pj}(t) = EF_{pj}(t_0) + p_{pj} A_4 (s_{pj}(t) - s_{pj}(t_0)) \quad (87)$$

for the projectile.

Then the total energy of the system is

$$E_T = E_{L1} + E_p + E_{L2} + E_{G2} + E_{L4} + E_{G4} + E_{K_{ps}} + \quad (88)$$

$$E_{K_{pj}} + E_{K_{L4}} + E_{K_{G4}} + E_{H4} + E_{F_{ps}} + E_{F_{pj}} .$$

This should be constant throughout the integration. In practice, energy errors of up to 0.5% have been observed. There is a small error in the liquid representation. As the liquid is compressed, the temperature will rise slightly, leading to a larger internal energy. This effect is ignored in the model. Other small errors are introduced by the approximations used for the heat and frictional losses.

## XX. NUMERICAL METHOD

Because of the length (about 75 pages) the code listing is not given. Appendix A lists the comments from the beginning of the code. This is a complete description of the input options and the notation actually used in the code for the input variables. A copy of the code is available from the author on request.

The ordinary differential equations derived above are solved using EPISODE.<sup>17</sup> This is a robust and efficient code for the solution of ordinary differential equations. The procedure is discussed in the previous reports.

## XXI. GE 30MM GUN FIXTURE

As an example of the procedure for using the gun code, a fixture developed by GE will be modeled. The purpose of this specific gun design was to show that a liquid propellant regenerative gun can operate in the high performance regime required for tank cannons. The fixture has so far only been fired with a 1/2 charge, since problems arose during the test sequence.<sup>4</sup> A schematic of the fixture is shown in Figure 2. Figure 3 shows the experimental chamber and liquid pressures, and Figure 4 the piston travel (Round 4). These

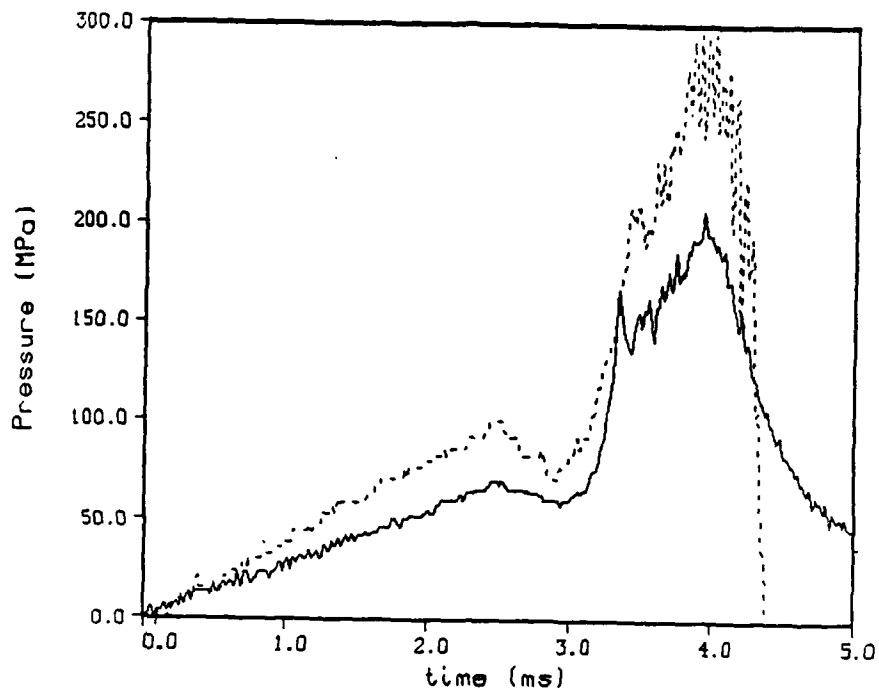


Figure 3. Experimental Chamber Pressure (line) and Liquid Pressure (dot) - Round 4.

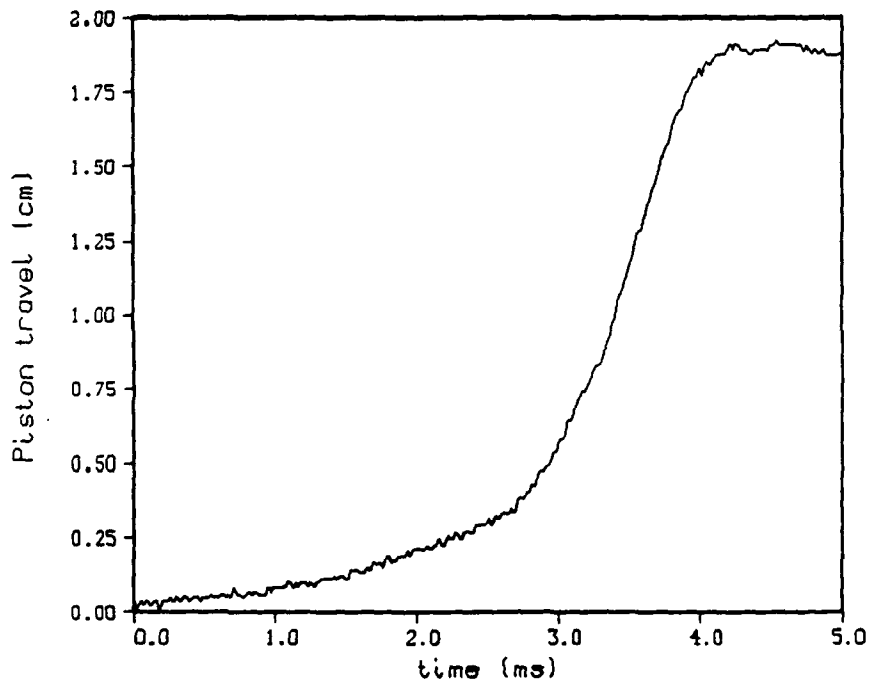


Figure 4. Experimental Piston Travel - Round 4.

profiles will be analyzed in detail below. All the data discussed in this report has been filtered to remove high frequency oscillations.

In a previous report<sup>12</sup> test data from an in-line regenerative gun was analyzed using an inverse code. Values of the discharge coefficient were derived. The discharge coefficient started small and took several milliseconds to rise to a value near one. A similar analysis was performed for the reverse gun. The vent area after shot start was computed based on the experimental projectile and piston travels. The vent area before shot start (through the tail seal) was chosen on the basis of agreement with the model. The liquid pressure measurement breaks down before the end of the firing cycle, so the liquid pressure is approximated as the chamber pressure times the hydraulic difference. In this case, where the vent area varies rapidly, it is more informative to plot the discharge coefficient times the vent area (effective area).<sup>18</sup> Figure 5 compares the calculated actual area with the derived effective area. After shot start, the discharge coefficient increases

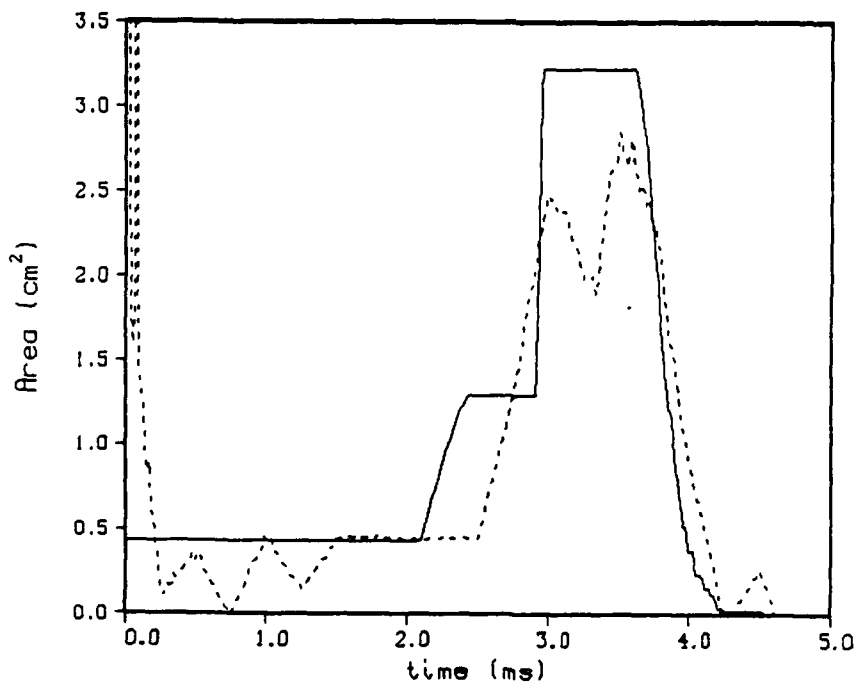


Figure 5. Actual Vent Area (line). Effective Area (dot). Round 4.

much more rapidly than for the in-line gun. But after the vents are fully open, the discharge coefficient (effective area) decreases before increasing close to the actual area. However, this decrease occurs at the point where the experimental chamber pressure is increasing very rapidly (see below). As a result, the pressures will not have time to equilibrate. The pressure measured near the wall of the chamber will not be equal to the actual pressure at the outlet of the injectors, and the liquid pressure will not equal the gun tube pressure times the hydraulic difference. Because of these effects, initially an attempt is made to model the data assuming a large constant discharge coefficient.

#### A. DESCRIPTION OF THE INPUT

Below is a description of the input for the gun code. This follows the format in Appendix A.

The first line is merely a label for the problem. It lists the filename of the input job stream and a brief description of the problem.

The initial offset of the projectile and the total distance traveled by the projectile before muzzle exit are given. The offset is chosen as the distance from the start of the short barrel to the start of the projectile. The diameter of the gun tube is given. The projectile and piston weights are entered (measured).

The initial volumes of the reservoir and chamber are given. The reservoir volume is computed from the drawings. The volume in the injection ports is ignored. The initial chamber volume is more complicated because of the slots in the stub case holder and the short barrel. A measurement was made of the volume from the stub case holder back by filling the assembly with water.<sup>19</sup> The rest of the volume is computed. The initial gun tube volume (computed as the projectile offset times the tube area) is subtracted from the total gas volume.

The areas of the piston on the reservoir and chamber sides are given, as well as the grease dyke area. The gun tube area is computed from the gun tube diameter.

The vent area in the piston is zero. The area between the chamber and the gun tube is estimated from the engineering drawings.

The areas of the three sets of holes are given. Each set consists of twelve holes. The length of the holes is only necessary if the transient injection model is used.

The offset is given from the initial position of the piston to the center of the piston side injection holes. This is just the maximum piston travel minus the radius of the holes. As the piston covers these holes, the injection area will be reduced.

The offset from the start of the tube to the center of both sets of tube side holes are given. The distance to the first set of holes is chosen so that the vents are just slightly open. The value was chosen to match the early piston travel. The distance to the first set of holes to the second set was read off the engineering drawings.

The piston resistance is taken to be uniformly zero. The discharge coefficient is set at a constant 0.95. This agrees well with higher dimensional transient models.<sup>5</sup>

The flow into the gun tube is normally modeled as steady state Bernoulli flow (FLUX1). The flow into the gun tube is steady state isentropic flow (FLUX1).

The nominal shot start pressure is 70 MPa, based on the strength of the break link. The experimental data shows that the projectile moves slightly sooner, and a value of 65 MPa is used. After shot start the resistance pressure is taken as 5 MPa. This is a typical value from

solid propellant gun modeling.

Next the physical properties of the propellant HAN1845 are given. The density at atmospheric pressure has been measured<sup>8</sup> and the bulk modulus has been fitted.<sup>7</sup> The chemical energy, the ratios of specific heats, the molecular weight of the propellant final products gas, and the covolume have been computed using BLAKE.<sup>9</sup> The surface tension and the kinematic viscosity of the liquid<sup>8</sup> are not actually required, but are used to compute the Weber number, the Reynold's number, and the third Lagrange number.

The liquid is pre-presurized to about 1 MPa. The gas is initially at one atmosphere.

As a first approximation, the liquid is assumed to combust instantaneously as it enters the combustion chamber (DROPl). Later the effects of accumulation will be studied.

The primer is assumed to be injected in the form of hot gas (PRIM3). There are 3.0 grams of IMR powder in the booster. Experiments with just the primer (water and dry shots) show an injection time of 1.5 ms. The heat loss was chosen to obtain a pressure due to the primer between the water and dry shot results.

Heat loss to the gun tube walls is calculated. The gun tube wall temperature is taken to be 300K. The heat loss algorithm in the code is not adjusted.

The air shock in front of the projectile is calculated. The air in the tube is initially assumed to be at 1 atm. and 300K. The values of the molecular weight and ratio of specific heats are taken at these conditions.

The standard Lagrange pressure distribution in the gun tube is

assumed.

The code will print out results every 0.05 ms. (TINC). Because the code must often change the time step, it is more efficient to restrict the maximum time step (HTOP). The error controls EPS and SREC are given typical values.

The integration method flag MF is set to 22 (backwards differentiation formulas with an internally computed Jacobian). KWRITE is set to zero to eliminate diagnostic messages. A time limit TMAX is set. If the code takes longer than TMAX seconds to execute, the code will stop and write the usual summary pages so all the information will not be lost. The code is only to be integrated once (REP1) and the chamber pressure will be computed normally (CHAM1).

An earlier version of these computations was presented at a JANNAF meeting.<sup>20</sup> The input used at that time was somewhat different. The hardware for this fixture recently arrived at BRL, and was somewhat different than the engineering drawings. Also, there was an error in the earlier calculation of the initial gas volume. The primary difference between this and the previous calculations is the smaller initial gas volume. Also, the grease dyke is smaller than in the previous calculations, which causes a larger hydraulic difference.

#### B. PRELIMINARY RUN

A preliminary run is made using the experimental chamber pressure (CHAM3). For numerical reasons, a spline fit of the pressure is used instead of the raw data (see Figure 6). The initial projectile offset is adjusted to match the early piston travel. Figure 7 shows the resulting piston travel. The agreement is quite good. Unlike the in-line gun,<sup>2</sup> a constant large discharge coefficient is a good approximation.

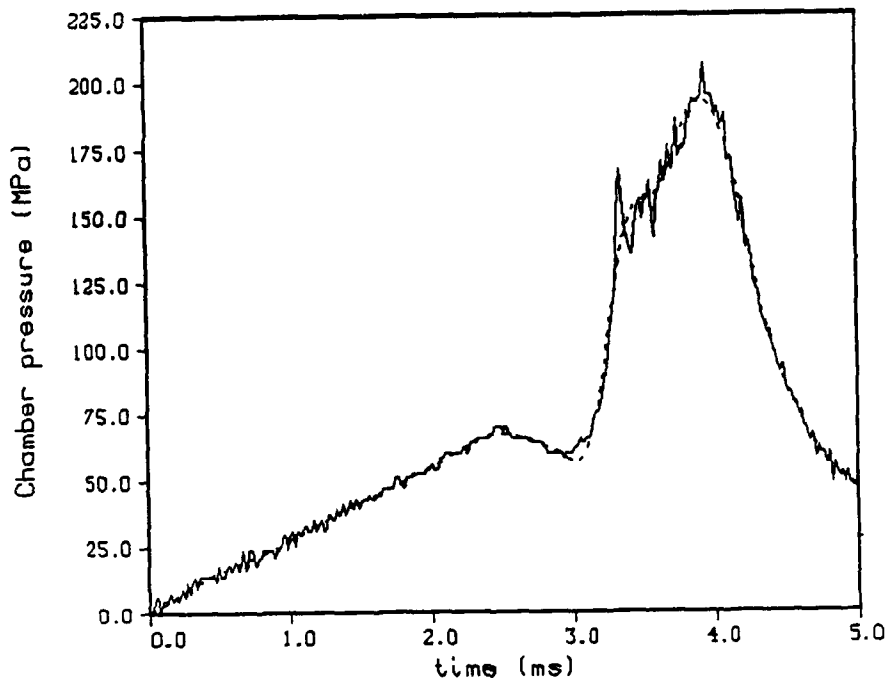


Figure 6. Experimental Chamber Pressure - Round 4 (line).  
Spline Fit to the Chamber Pressure (dot).

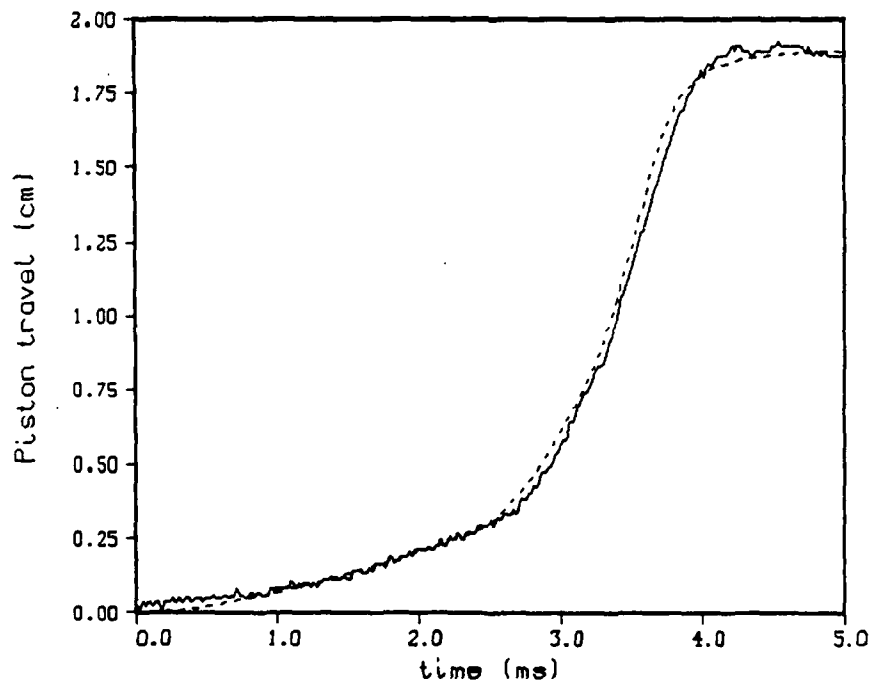


Figure 7. Experimental Piston Travel - Round 4 (line).  
Model with Experimental Chamber Pressure (dot).

The effect of recoil is a possible problem. The piston travel was measured in a relative sense. The data is normalized to the maximum piston travel. However, the gun recoil is not measured. To estimate the size of this effect, the recoil is computed based on the forces acting on the gun. The weight of the gun is estimated from its volume.<sup>19</sup> Since the recoil mechanism has not been studied, free recoil is assumed. The computed recoil will then be larger than the actual recoil. Figure 8 shows the computed recoil, compared to the experimental and model piston travel. Recoil does not begin to be important until near the end of the piston stroke. The model shows a very slow approach by the piston to the end of the reservoir. The experiment instead shows a small reversal. The size of this reversal is in reasonable agreement with the computed recoil. The later and much faster reversal cannot be due to recoil, and must instead be actual piston motion. The final result is that the experimental piston travel is slightly too large. The effect is small, and no attempt is made to correct for the effect of recoil. Since the mount restricts the recoil, the actual error due to recoil is very small.

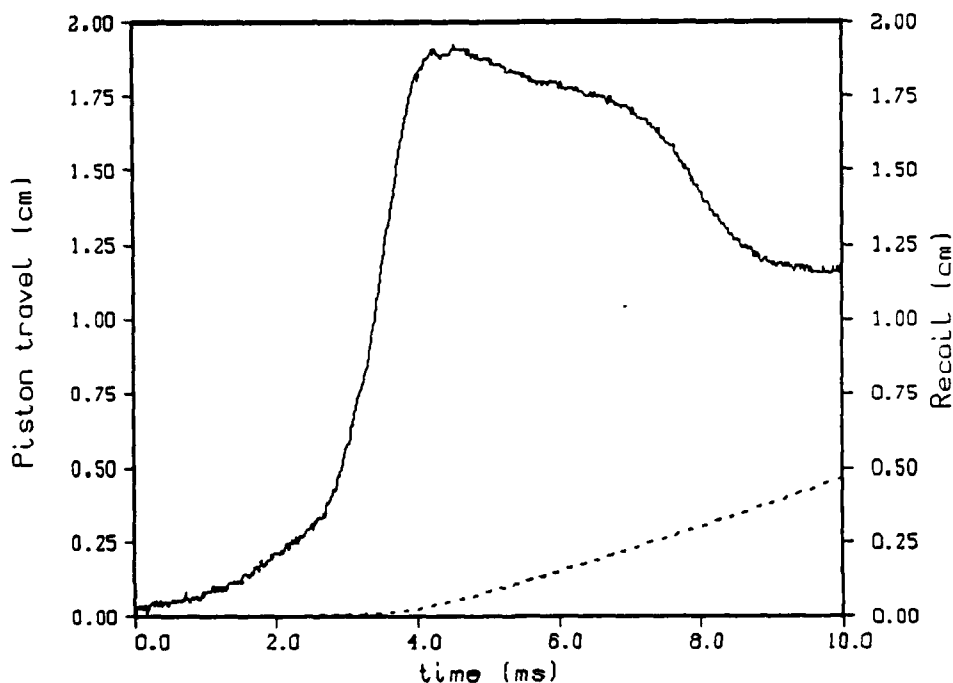


Figure 8. Experimental Piston Travel - Round 4 (line).  
Computed Gun Recoil (dot).

The muzzle velocity predicted by the code is more than 10% high. The Lagrange pressure distribution is derived under the assumption that the pressure equilibrates instantly in the gun tube. In the case considered here, the pressure increase is too rapid, and the pressure at the base of the projectile will be lower than that predicted by the Lagrange distribution (see below).

In earlier work on this fixture by Bulman and Maher<sup>21</sup>, a low effective area (discharge coefficient) was blamed for the delayed propellant ignition. Poor flow through the "Y" shaped passages was considered to be the major problem, rather than liquid accumulation. This is opposite the conclusion reached in this paper. As a partial check, the code was run still using the experimental chamber pressure but assuming a discharge coefficient of 0.85 and 0.75 (Figure 9). The initial projectile offset was adjusted slightly for the two new cases to match the early piston travel. There is not a great deal of difference in the profiles. As mentioned above, the experimental piston travel is

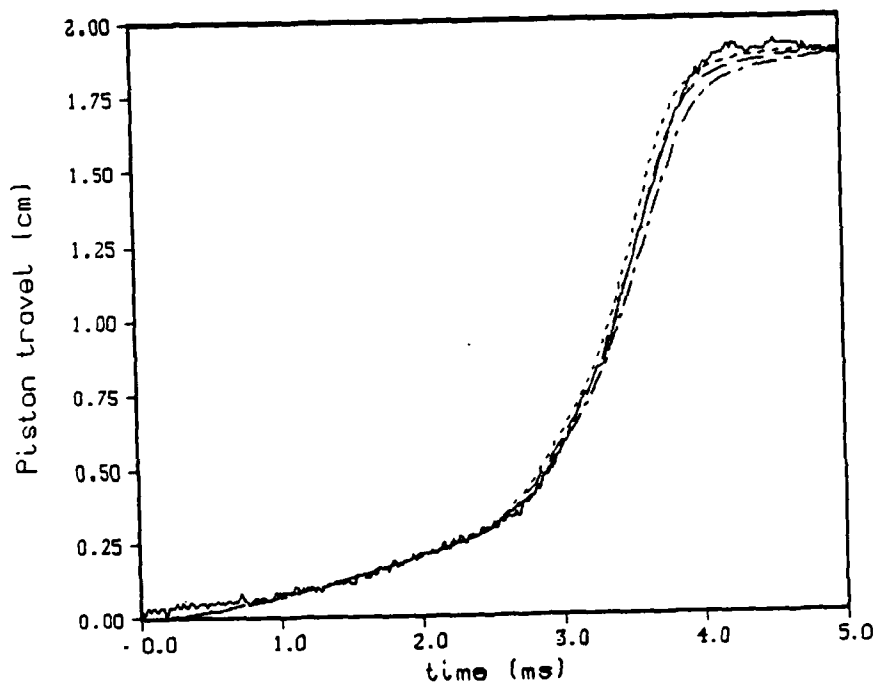


Figure 9. Experimental Piston Travel - Round 4 (line). Model with Experimental Chamber Pressure.  $C_D = 0.95$  (dot).  $C_D = 0.85$  (dash).  $C_D = 0.75$  (dot-dash).

not known completely accurately. Also, the pressure rise is too rapid for the system to equilibrate. The pressure at the injection holes outlet will probably be higher in reality than in the model, leading to a lower apparent discharge coefficient. So the value of 0.95 is still thought to be the best approximation to the system. However, there may be minor flow problems in the "Y" shaped passages.

#### C. MODELING - ROUNDS 4-10

The model is used to compute the pressure, assuming instantaneous burning. Figures 10 and 11 show the results. To make comparisons more easily, the model curves have been shifted uniformly in time so the chamber pressures match at 75 MPa. The agreement is very poor. This run shows that liquid accumulation plays a major role in the fixture. However, this model does reproduce the first part of the rapid chamber pressure rise.

The droplet option was introduced next. The drop size versus projectile travel table was adjusted by trial and error until reasonable agreement with the chamber pressure was obtained. The change from the DROPl option to DROp4 is the only change made in the code. The results (Figures 12-13) no longer require centering, since the delay in the experimental pressure rise is now being modeled. The agreement with the experimental data is quite good. Figure 14 shows the droplet diameter, and Figure 15 the calculated liquid accumulation in the chamber/ gun tube.

Appendix B shows the input for this run. The numbers and labels at the left are read by the code. The comments at the right are for user identification. The corresponding output is also given. The code was run on the BRL Cray-2. The input is echoed back, along with other calculated initial values. Once the integration begins, output is given every 0.05 ms. The pressures, piston travel and velocity, and projectile travel and velocity are given. At the end of the

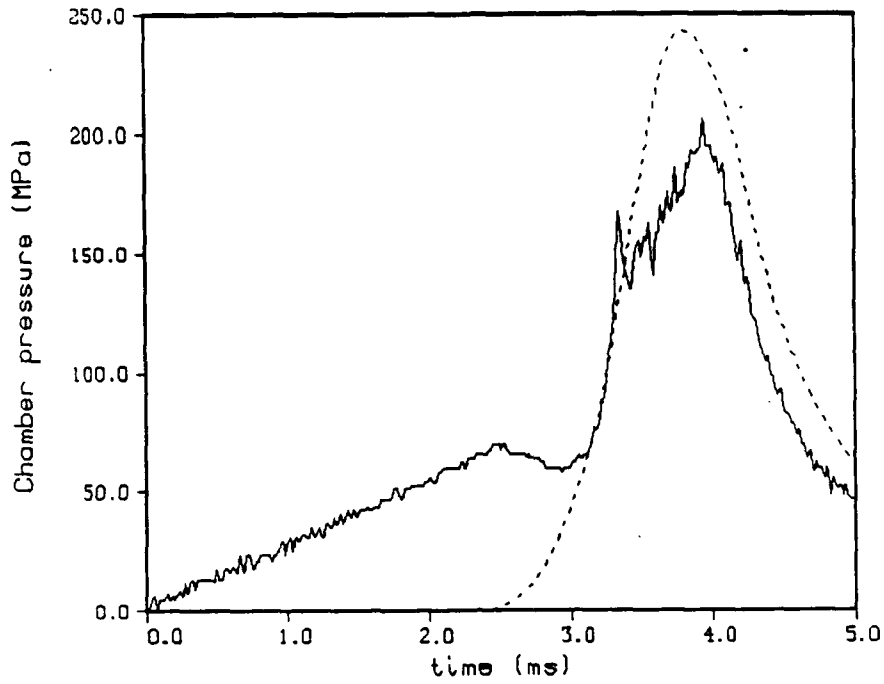


Figure 10. Experimental Chamber Pressure - Round 4 (line).  
Model - Instantaneous burning (dot).

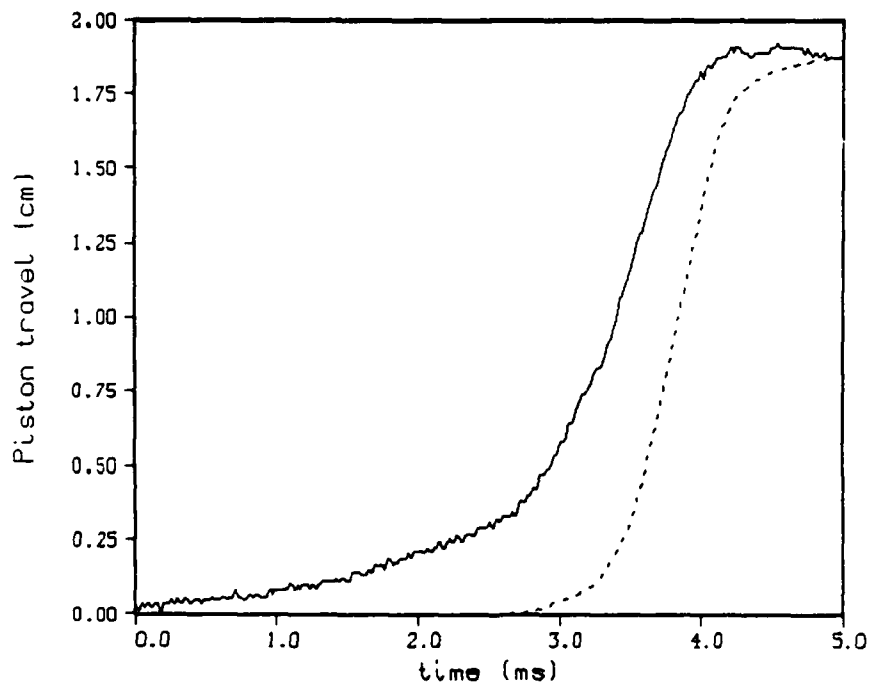


Figure 11. Experimental Piston Travel - Round 4 (line).  
Model - Instantaneous burning (dot).

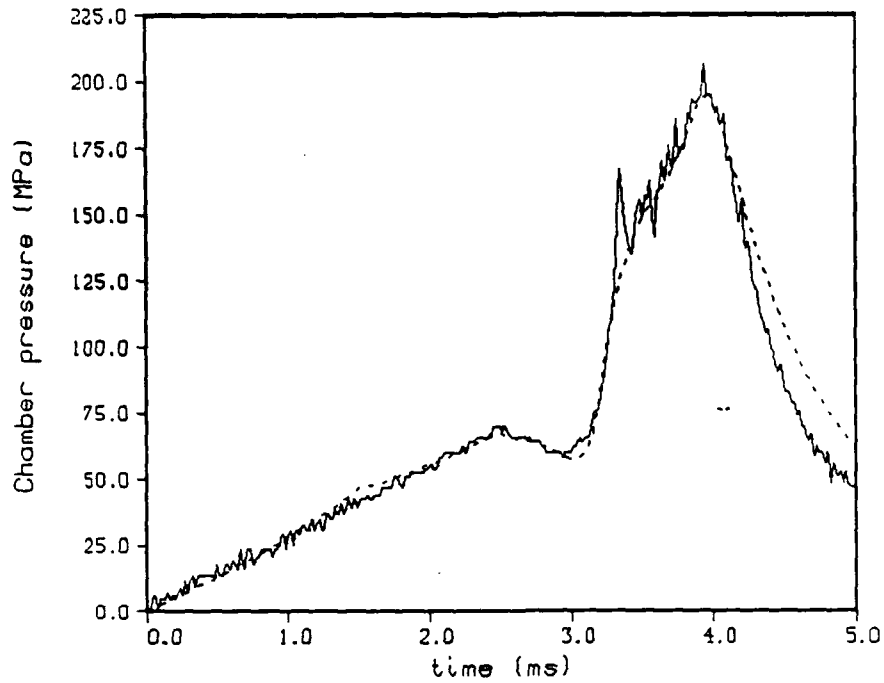


Figure 12. Experimental Chamber Pressure - Round 4 (line).  
Model - Droplet burning (dot).

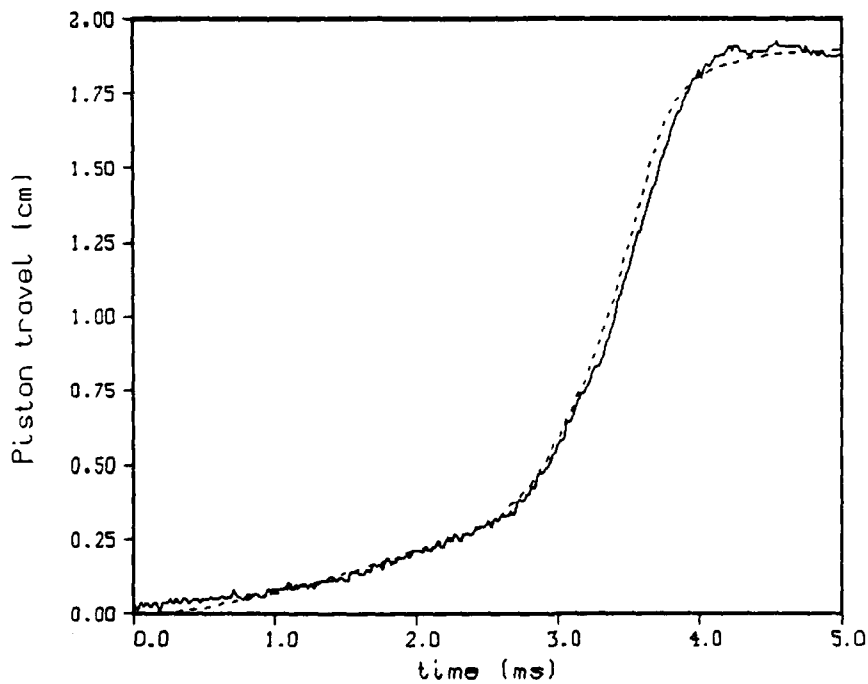


Figure 13. Experimental Piston Travel - Round 4 (line).  
Model - Droplet burning (dot).

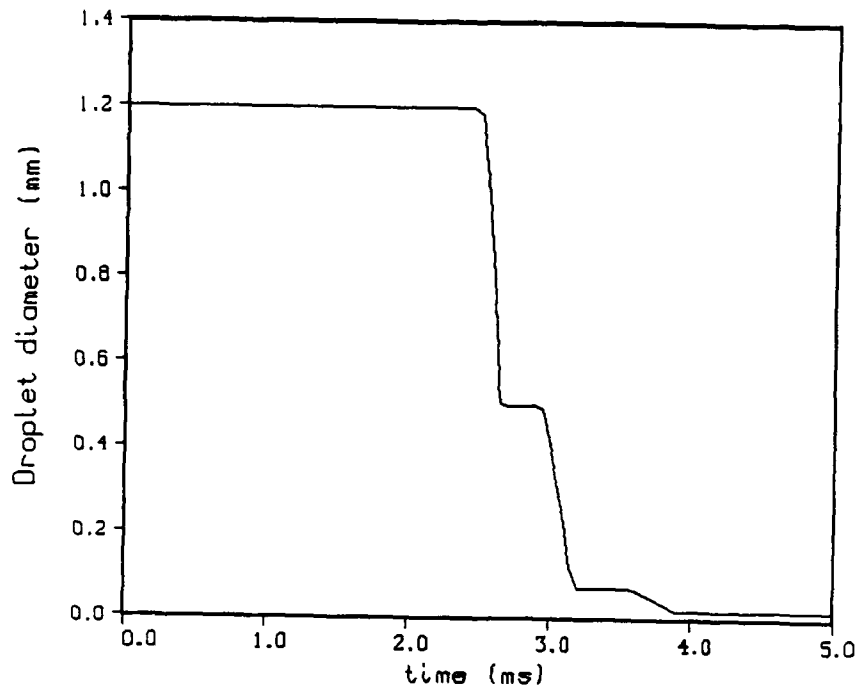


Figure 14. Model - Droplet Diameter - Round 4.

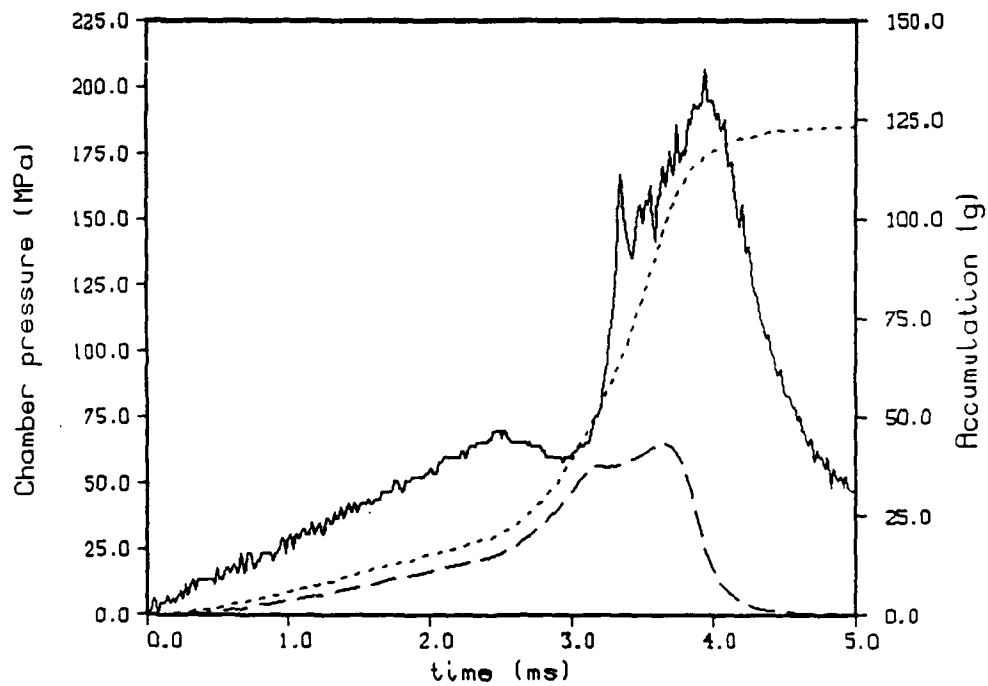


Figure 15. Experimental Chamber Pressure - Round 4 (line). Mass in the Chamber/ Gun Tube (dot). Liquid Accumulation (dash).

integration, a summary page is given. A second page shows when various maximum values are achieved. There are many other variables of interest in the simulation. As the integration proceeds, these are written onto other files, and can be appended to the output. In Appendix B, only the minimal output is given.

Now consider the profiles in more detail. The primer causes the initial pressure rise. Liquid is then injected slowly around the tail seal on the projectile. According to the model, only about 1/5 of the liquid injected before shot start actually combusts. At about 65 MPa, the shot start link releases. The pressure now decreases. The rapid projectile motion opens the vents completely. It also causes the hot gas to cool by isentropic expansion. The cold liquid propellant suddenly is injected into the cooler gas and quenches the combustion. Combustion is almost negligibly small. Since liquid is being injected rapidly, the liquid accumulation becomes large (about 1/3 of the original charge). Eventually the liquid reignites, causing a very rapid pressure rise. The measured chamber pressure increases 90 MPa in 0.14 ms. The pressure increase in the gun tube itself is not measured, and may be even more steep. Combustion is so rapid compared to the speed of sound that large pressure gradients will be created. The model assumptions of uniform pressure in the chamber and a Lagrange pressure distribution in the gun tube are not accurate.

Only a small amount of the accumulation burns off at this time. The experiment does show a higher pressure rise than the model, so more liquid will be burned off in practice. However, a large part of the pressure rise is injection driven. The local pressure rises so rapidly that the liquid pressure does not have time to equilibrate. The local gun tube pressure than can become as large as the liquid pressure (see Figure 3) and injection is shut off. The chamber pressure than falls steeply, since the combustion is largely injection driven. The pressure shows low frequency oscillations for the rest of stroke. Since the model assumes that pressures equilibrate instantly, it does not reproduce this

behavior.

The piston then moves over the injection holes. This causes a rapid deceleration of the piston. Only near the end of the injection process does most of the accumulation burn off. Eventually the hot gas propagates back into the reservoir. In this case, there is very little liquid left, and the reversal is very mild, as shown in Figure 8 at about 7 ms.

Two other shots (Rounds 7 and 8) gave results similar to Round 4. For Round 6, the break link released prematurely. Due to the lower pressure, the liquid never reignited (flameout).

Round 10 is similar to Round 4 (see Figure 16). However, there was an even longer delay before the liquid reignited. The resulting chamber pressure rise was very rapid (150 MPa in 0.04 ms). There was a piston reversal during this steep pressure rise, although blow-out plugs

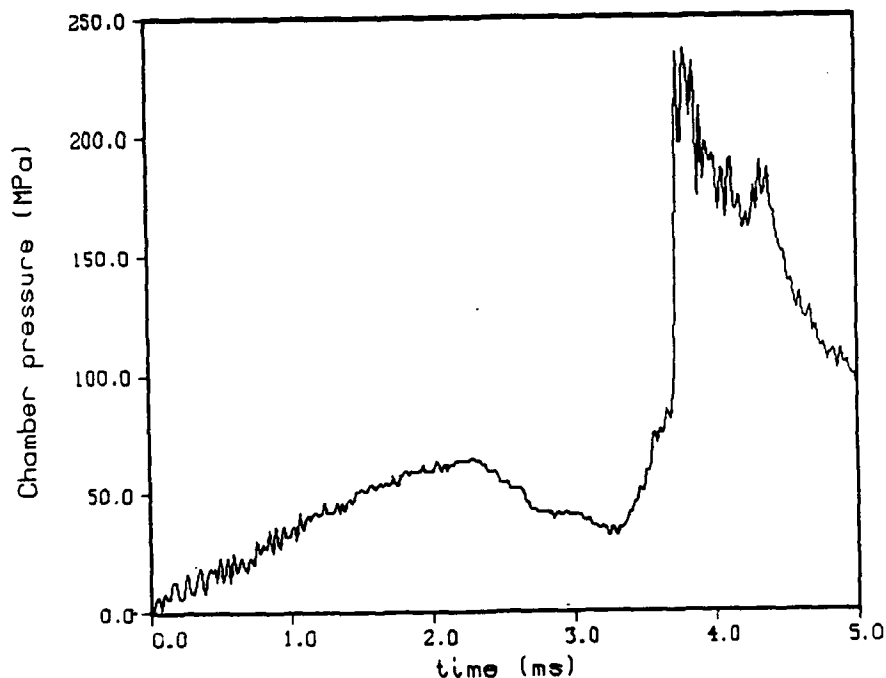


Figure 16. Experimental Chamber Pressure - Round 10.

in the reservoir prevented damage to the system. Since most of the combustion takes place in the tube, the gun tube pressure became much higher than the chamber pressure at the piston, and even higher than the liquid pressure. Hot gas then easily enters the reservoir and causes the piston reversal.

The major problem with this fixture is the large liquid accumulation. This can lead to flameout, or to a very rapid pressure rise if the liquid reignites. The pressure rise will be rapid even without accumulation (see Figure 10), because the initial gas volume is small. However, a rapid local pressure rise will shut off the injection. The presence of accumulated liquid allows the pressure to keep increasing after injection has stopped, causing the back flow and the piston reversal.

#### D. MODELING - ROUNDS 25-28

An earlier fixture, also without injection through the piston, was more successful.<sup>18</sup> The present fixture was modified to bring it closer to the previous design. The injection area was cut in half. The forward and backward holes were staggered, instead of meeting at a "Y". The projectile mass was increased to 350 grams. A different break link was used, with a shot start of 45 MPa. The break link also stretched, leading to a proportionally larger initial injection area. Slightly less primer was used.

Figures 17 and 18 show the experimental data for Round 25. There is no longer a delay in the pressure rise after shot start. It is harder to compare the piston travel because recoil is more important for this design. Because of the heavier projectile and hence lower velocity, higher pressures are exerted for a longer period of time.

As before, a preliminary run was made using the experimental chamber pressure (CHAM2 option). The agreement with the experimental

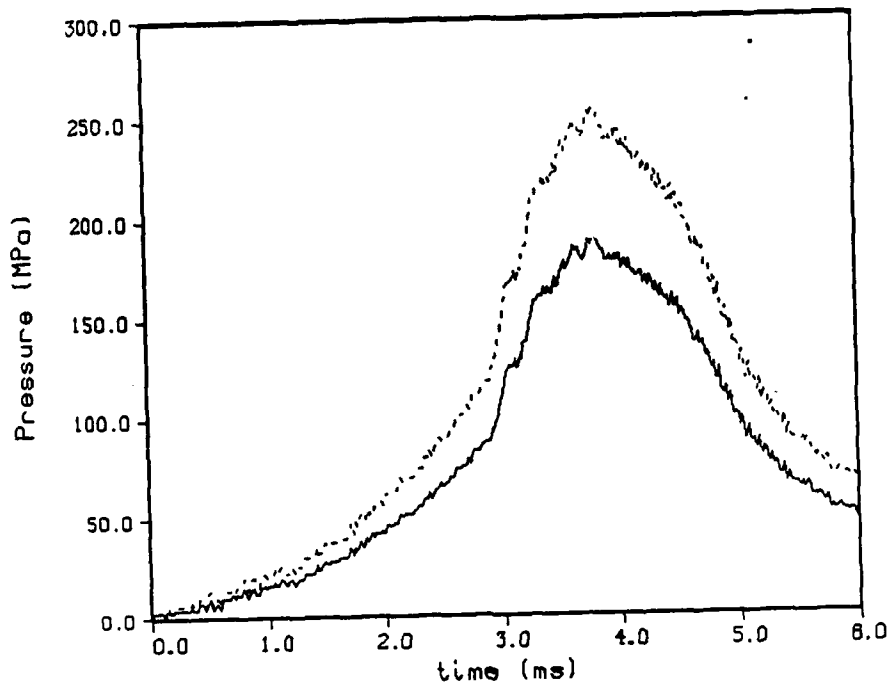


Figure 17. Experimental Chamber Pressure (line) and Liquid Pressure (dot) - Round 25.

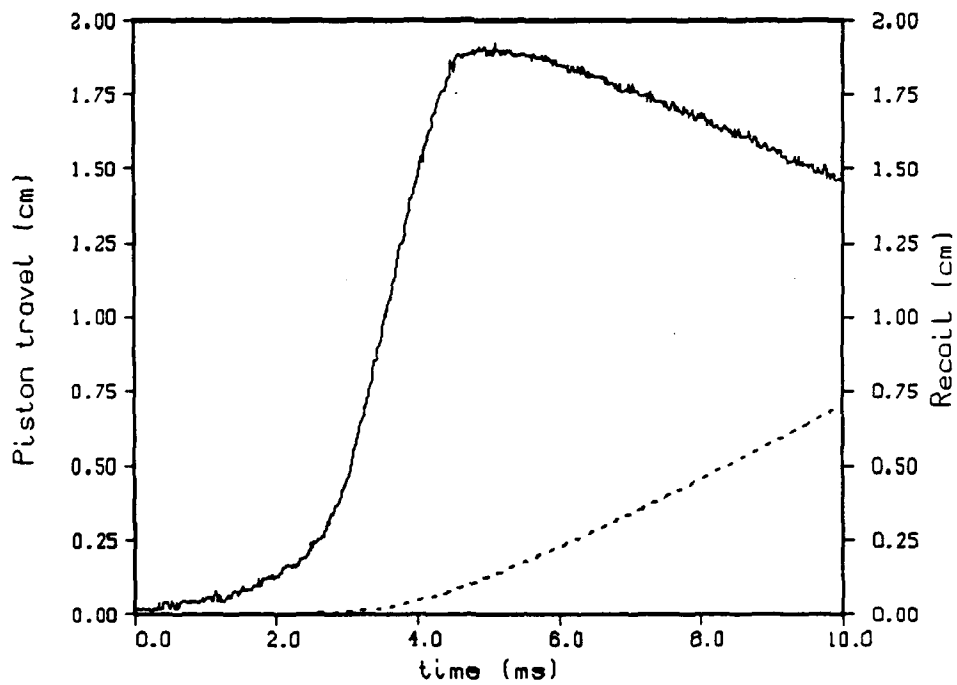


Figure 18. Experimental Piston Travel (line) and Computed Recoil (dot) - Round 25.

muzzle velocity is now very good. The Lagrange pressure distribution is adequate if the pressure rise is not too rapid.

Using the droplet option, this case can be modeled more simply than Round 4. Appendix C gives the input and the summary page for the output. Combustion is still inefficient at first. But when the projectile starts to move, the liquid is injected slowly enough so that relatively little accumulation occurs (Figures 19-22). The agreement in piston travel is good. If the experimental piston travel could be corrected for recoil, the agreement would probably improve. This cannot presently be done because the effect of the mount on the actual recoil is unknown.

The experiment still shows a rapid pressure rise just before 3.0 ms. This occurs right after the projectile clears the injection holes. Since the projectile is much heavier and the shot start is lower, there is more of a delay between shot start and the opening of the injectors. The pressure increases rapidly for a short time and then levels off. The pressure rise is as before too rapid for the liquid pressure to equilibrate. The rapid local pressure rise slows down dramatically the injection rate. The accumulation is not burning off at this point, so when the injection rate becomes slow enough, the pressure stops increasing. This occurs at least once more before peak pressure. The model, since it assumes that the pressures equilibrate, does not demonstrate this behavior.

Rounds 26 and 27 were very similar to Round 25. However, Round 28 showed a piston reversal. The reversal occurred soon after the peak pressure, as the piston was just starting to block off the injection holes. The piston actually starts to decelerate compared with the model right after the projectile clears the injection ports. At this point the chamber pressure goes up rapidly compared to Round 25 (40 MPa in 0.1 ms). The recorded chamber pressure is essentially equal to the recorded liquid pressure, and the gun tube pressure should be higher than the

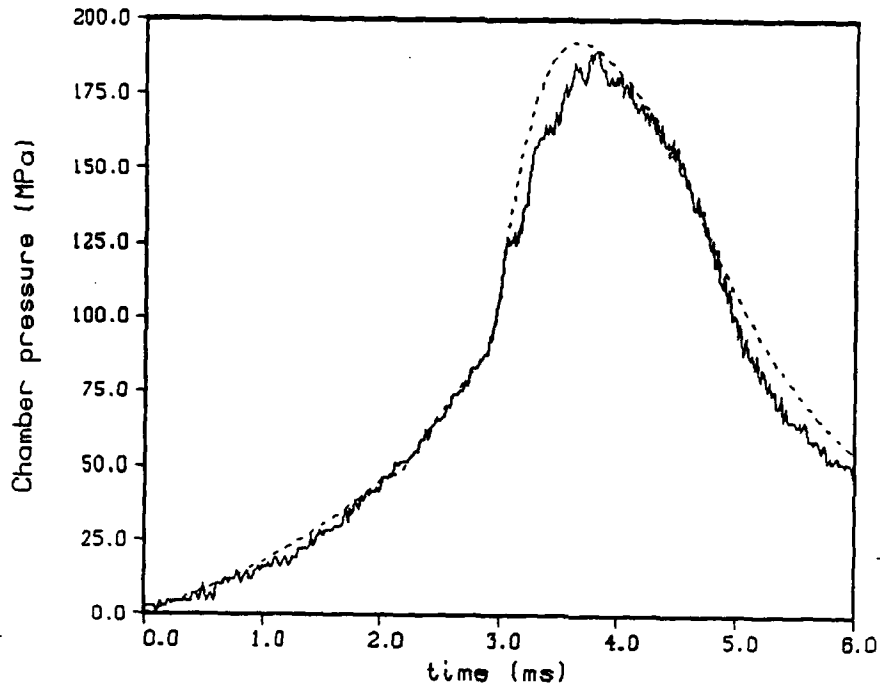


Figure 19. Experimental Chamber Pressure - Round 25 (line).  
Model - Droplet Burning (dot).

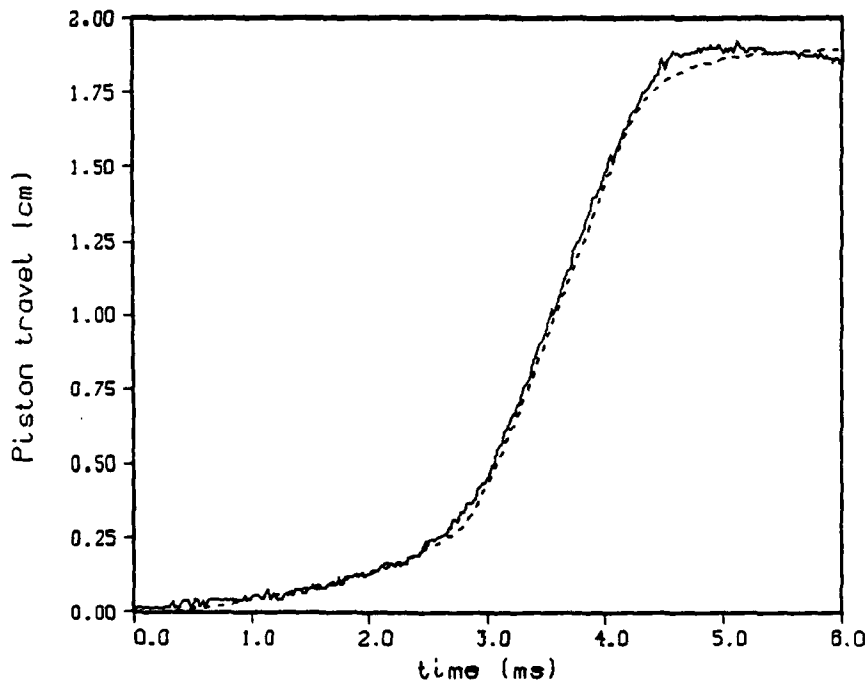


Figure 20. Experimental Piston Travel - Round 25 (line).  
Model - Droplet Burning (dot).

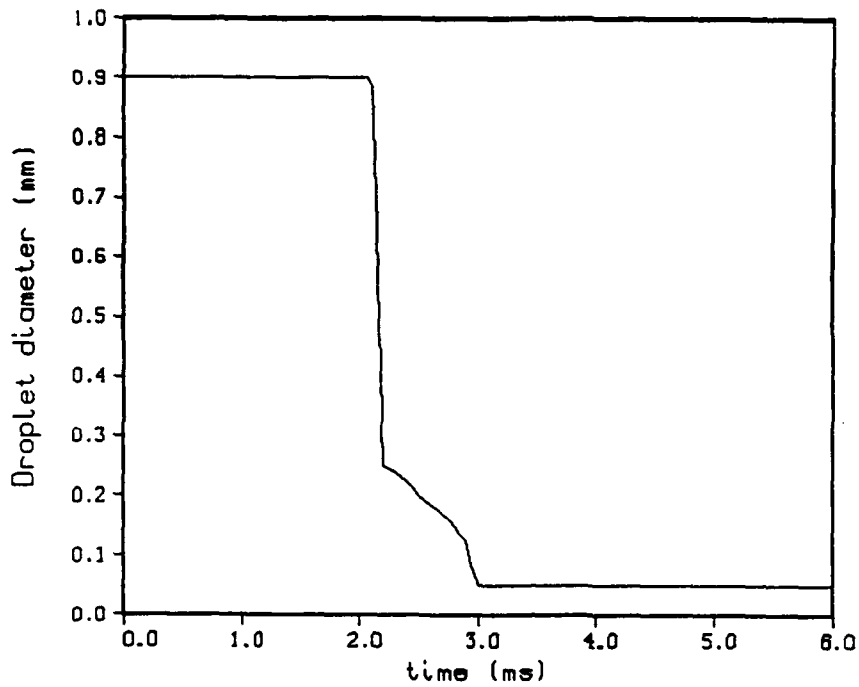


Figure 21. Model - Droplet Diameter - Round 25.

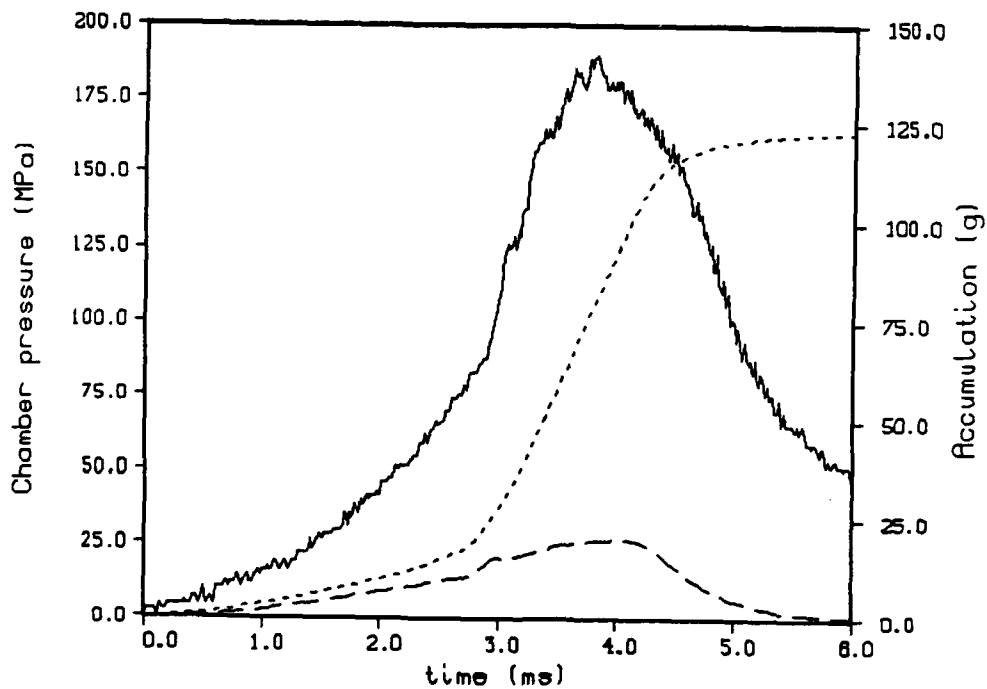


Figure 22. Experimental Chamber Pressure - Round 25 (line). Mass in the Chamber/ Gun tube (dot). Liquid Accumulation (dash).

chamber pressure (see Figure 23). Hot gas then could start to back up into the injection ports. The pressure rise is much less dramatic than for Round 10, and the corresponding piston reversal is more gradual.

The initial pressure rise (before shot start) is more rapid here than for Round 25, implying more efficient combustion. The same injection driven pressure rise occurs when the projectile opens the injection ports. However, in this case a small amount of the accumulated liquid also burns, pushing the pressure high enough to cause the gas backup.

There is another important point here. Since there is no longer a quenching period before the rapid pressure rise, the volume is only slightly larger than the initial very small gas volume of  $50 \text{ cm}^3$  when the pressure rise occurs. It then takes less combustion to cause a given pressure rise. It is easier to cause a rapid pressure rise and gas backup.

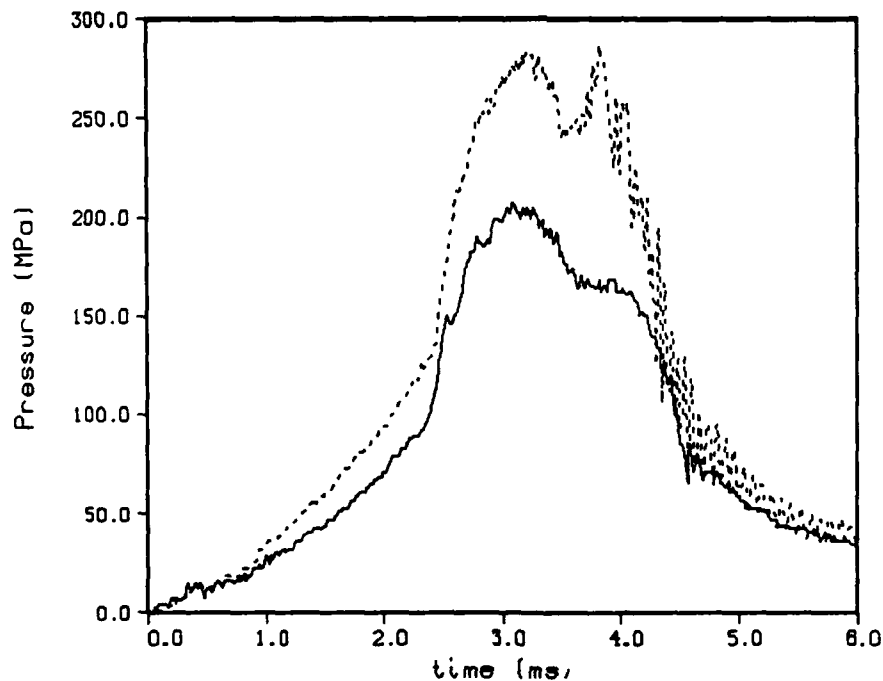


Figure 23. Experimental Chamber Pressure (line) and Liquid Pressure (dot) - Round 28.

The previous gun fixture did not exhibit the same problems with piston reversal.<sup>18</sup> However, the earlier fixture had a larger hydraulic difference. The liquid pressure would be higher compared to the gun tube pressure, making a reversal less likely.

#### E. DISCUSSION

The experimental data can be reproduced accurately using the model. Assuming a large constant discharge coefficient is a good approximation, unlike the in-line case. However, liquid accumulation is very important, especially for the larger injection area.

The major problem with this design is the rapid injection of liquid into a small volume as the projectile first starts to move. This may totally quench the combustion, causing a flameout, or it may temporarily quench the combustion. When the liquid reignites, the very rapid pressure increase leads to non-uniform pressure and a possible dramatic piston reversal. Even if the combustion does not quench, the rapid injection leads to a rapid pressure increase. Again, the non-uniform pressure allows hot gas to penetrate into the reservoir, in this case causing a much milder piston reversal.

The fixture is designed to reach high muzzle velocities. This implies that liquid must be injected rapidly. As the fixture moves closer to the high performance regime, the problems can be expected to get worse.

One previous suggestion is a multi-angle injector.<sup>4</sup> The liquid would be introduced somewhat more gradually and would be spread out more along the gun tube. The fixture would be more complicated. And since the projectile moves rapidly at shot start, all the injection ports would be opened very quickly.

A simpler idea is to change the design of the booster and/or the

tail seal.<sup>19</sup> At present the hot igniter gases are aimed directly at the piston. Meanwhile, cold liquid is injected around the tail seal and directed along the wall of the short barrel. The model shows that very little of this liquid burns. Since it will be cooled by contact with the wall, this is not surprising. Some of the holes in the booster could be redirected toward the wall of the short barrel. This would tend to ignite the liquid and prevent the early accumulation. In addition, the tail seal could be redesigned to direct the liquid toward the center of the gun tube rather than along the walls. If the liquid can be ignited early, the combustion is not likely to be quenched when the main injection process begins.

Even if the quenching phase is eliminated, this may not completely solve the problem, as Round 28 shows. There can be a rapid pressure rise even with very little accumulation. The initial gas volume could be made larger, which would make it harder for the pressure to rise rapidly. Also, the piston could be redesigned to obtain a larger hydraulic difference. If the liquid pressure is designed to be higher relative to the chamber pressure, gas backup into the reservoir becomes less likely.

As a last resort, some of the liquid could be injected through the piston. This was done for most of the earlier tests conducted with this type of fixture.<sup>18</sup> With propellant burning directly outside the reservoir, the liquid pressure will stay higher. Also, if the fixture is designed so there is gas flow out of the chamber into the tube, this will tend to break up liquid concentrations near the gun tube injection holes. However, this would complicate the fixture considerably.

## XXII. CONCLUSIONS

A description is given of a lumped parameter model for reverse annular regenerative liquid propellant guns. A complete discussion of the governing equations and the different options is given. The code

has been used to test the effect of various assumptions, so additional options will be added as needed.

The model results are compared with experimental data from a 30mm gun fixture. A discussion is given of the procedure for choosing a set of input parameters. Assuming a large steady discharge coefficient is a good approximation, unlike the case of in-line guns. By assuming instantaneous burning, the overall performance of the gun can be predicted with reasonable accuracy.

Liquid accumulation is very important for this fixture. This cannot be predicted, since the flow fields and combustion are not well understood, but the code can be adjusted to match a given experiment. The code can then be used to study details not available from the experiment.

This particular fixture exhibits difficulties. Just after shot start there can be excessive liquid accumulation, quenching the flame. After the maximum pressure there can be piston reversal. Neither effect can be predicted by the lumped parameter code, but the model results help explore different hypotheses for this behavior.

## REFERENCES

1. Coffee, T.P., "A Lumped Parameter Code for Regenerative Liquid Propellant Guns," BRL-TR-2703, December 1985.
2. Coffee, T.P., "An Updated Lumped Parameter Code for Regenerative Liquid Propellant In-Line Guns," BRL-TR-2974, December 1988.
3. Gough, P.S., "A Model of the Interior Ballistics of Hybrid Liquid-Propellant Guns," Contract Report BRL-CR-566, March 1987.
4. Watson, C., Knapton, J.D., Morrison, W.F., and Maher, D., "Ballistic Investigations of a High Performance Regenerative Liquid Propellant Gun," BRL report, to be published.
5. Coffee, T.P., "One-Dimensional Modeling of Liquid Injection in a Regenerative Propellant Gun," BRL-TR-2897, March 1988.
6. Corner, J., Theory of the Interior Ballistics of Guns, Wiley, New York, 1950.
7. Constantino, M., "The High Pressure Equations of State of LGP 1845 and LGP 1846," UCRL-93985, Preprint.
8. Decker, M.M., Klein, N., Freedman, E., Leveritt, C.S., and Wojciechowski, J.Q., "HAN-Based Liquid Gun Propellants: Physical Properties," BRL-TR-2864, November 1987.
9. Freedman, E., "BLAKE - A Thermodynamics Code Based on TIGER: Users' Guide and Manual," ARBRL-TR-02411, July 1982.
10. Sears, F.W., An Introduction to Thermodynamics, the Kinetic Theory of Gases, and Statistical Mechanics, 2nd ed., Addison-Wesley Publishing

Company, Inc., London, England, 1959.

11. Fox R.W., and McDonald, A.T., Introduction to Fluid Mechanics, 2nd ed., John Wiley and Sons, NY, 1978.

12. Coffee, T.P., "Injection Processes in Liquid Regenerative Propellant Guns," BRL-TR-2846, August 1987.

13. Morrison, W.F., and Coffee, T.P., "Modifications of the Lagrange Pressure Distribution for Liquid Propellant Guns," BRL report, to be published.

14. Nordheim, L.W., Soodak, H., and Nordheim, G., "Thermal Effects of Propellant Gases in Erosion Vents and in Guns," National Defense Research Committee, Armor and Ordnance Report No. A-262 (OSRD No. 3447), May 1944.

15. McBratney, W.F., "Windowed Chamber Investigation of the Burning Rate of Liquid Monopropellants for Guns," ARBRL-MR-03018, April 1980.

16. McBratney, W.F., "Burning Rate Data, LPG 1845," ARBRL-MR- 03128, August, 1981.

17. Hindmarsh, A.C., and Byrne, G.D., "EPISODE: An Effective Package for the Integration of Systems of Ordinary Differential Equations," UCID-30112-Rev.1, Lawrence Livermore Laboratory, 1977.

18. Bulman, M., "Regenerative Liquid Propellant Tank Guns," Preliminary Status Report, General Electric, August 1987.

19. Watson, C., BRL, Private Communication, 1988.

20. Coffee, T.P., "Analysis of a High Performance Regenerative Liquid Propellant Gun," 25th JANNAF Combustion Meeting, Huntsville, AL, October 1988.

21. Bulman, M., and Maher, D., GE, presentation at BRL, April 1987.

## GLOSSARY

- $A_1$  Area of the piston - liquid side,  $\text{cm}^2$ .
- $A_2$  Area of the piston - chamber side,  $\text{cm}^2$ .
- $A_4$  Area of the gun tube,  $\text{cm}^2$ .
- $A_g$  Area of the grease dyke around the piston,  $\text{cm}^2$ .
- $A_{12}$  Area of the vent into the chamber from the reservoir,  $\text{cm}^2$ .
- $A_{14}$  Area of the vent into the gun tube from the reservoir,  $\text{cm}^2$ .
- $b$  Covolume,  $\text{cm}^3/\text{g}$ .
- $c_1$  Speed of sound in the liquid in the reservoir,  $\text{cm}/\text{s}$ .
- $c_2$  Speed of sound in the mixture in the chamber,  $\text{cm}/\text{s}$ .
- $c_4$  Speed of sound in the mixture in the gun tube,  $\text{cm}/\text{s}$ .
- $c_{L2}$  Speed of sound in the liquid in the chamber,  $\text{cm}/\text{s}$ .
- $c_{L4}$  Speed of sound in the liquid in the gun tube,  $\text{cm}/\text{s}$ .
- $c_{G2}$  Speed of sound in the gas in the chamber,  $\text{cm}/\text{s}$ .
- $c_{G4}$  Average speed of sound in the gas in the gun tube,  $\text{cm}/\text{s}$ .
- $c_p$  Specific heat at constant pressure,  $\text{j}/\text{g}\cdot\text{K}$ .
- $c_v$  Specific heat at constant volume,  $\text{j}/\text{g}\cdot\text{K}$ .

$C_D$	Discharge coefficient for the mass flux from the reservoir.
$d_4$	Diameter of the gun tube, cm.
$e_1$	Chemical energy of the liquid, j/g.
$e_2$	Internal energy of the gas in the chamber, j/g.
$e_4$	Internal energy of the gas in the gun tube, j/g.
$E_{L1}$	Total internal energy in the liquid reservoir, j.
$E_{L2}$	Total internal energy in the liquid in the chamber, j.
$E_{L4}$	Total internal energy in the liquid in the gun tube, j.
$E_{G2}$	Total internal energy in the gas in the chamber, j.
$E_{G4}$	Total internal energy in the gas in the gun tube, j.
$E_p$	Total internal energy in the unburned primer, j.
$E_{K_{L4}}$	Kinetic energy of the liquid in the gun tube, j.
$E_{K_{G4}}$	Kinetic energy of the gas in the gun tube, j.
$E_{K_{pj}}$	Kinetic energy of the projectile, j.
$E_{K_{ps}}$	Kinetic energy of the piston, j.
$E_{H_4}$	Total heat loss to the gun tube walls, j.
$E_{F_{pj}}$	Total energy loss due to projectile friction, j.

$E_{F_{ps}}$  Total energy loss due to piston friction, j.  
 $E_T$  Total energy of the system, j.  
 $g_0$  Conversion constant =  $10^7$  g/MPa-cm-s<sup>2</sup>.  
 $h_{L1}$  Liquid enthalpy in the reservoir, j/g.  
 $h_{L2}$  Liquid enthalpy in the chamber, j/g.  
 $h_{L4}$  Liquid enthalpy in the gun tube, j/g.  
 $h_{G2}$  Gas enthalpy in the chamber, j/g.  
 $h_{G4}$  Gas enthalpy in the gun tube, j/g.  
 $h_w$  Heat transfer coefficient to the gun tube walls, j/cm<sup>2</sup>-K-s.  
 $K$  Bulk modulus, MPa.  
 $K_1$  Bulk modulus at zero pressure, MPa.  
 $K_2$  Derivative of the bulk modulus.  
 $m_{12}$  Mass flux from the reservoir into the chamber, g/s.  
 $m_{14}$  Mass flux from the reservoir into the gun tube, g/s.  
 $m_{24}$  Mass flux from the chamber into the gun tube, g/s.  
 $m_{p4}$  Mass flux of the primer into the gun tube, g/s.  
 $m_2$  Chamber rate of production of gas by combustion, g/s.

$m_4$  Gun tube rate of production of gas by combustion, g/s.  
 $m_{L2}$  Total rate of production of liquid in the chamber, g/s.  
 $m_{L4}$  Total rate of production of liquid in the gun tube, g/s.  
 $m_{G2}$  Total rate of production of gas in the chamber, g/s.  
 $m_{G4}$  Total rate of production of gas in the gun tube, g/s.  
 $M_1$  Total mass in the reservoir, g.  
 $M_2$  Total mass in the chamber, g.  
 $M_4$  Total mass in the gun tube, g.  
 $M_{L2}$  Liquid mass in the chamber, g.  
 $M_{L4}$  Liquid mass in the gun tube, g.  
 $M_{G2}$  Gas mass in the chamber, g.  
 $M_{G4}$  Gas mass in the gun tube, g.  
 $M_p$  Unburned primer mass, g.  
 $M_T$  Total propellant mass in the system, g.  
 $M_{pj}$  Mass of the projectile, g.  
 $M_{ps}$  Mass of the piston, g.  
 $M_g$  Molecular weight of the gas, g/mole.

$P_1$	Pressure in the liquid reservoir, MPa.
$P_2$	Pressure in the chamber, MPa.
$P_4$	Space mean pressure in the gun tube, MPa.
$P_L$	Pressure at the breech end of the gun tube, MPa.
$P_R$	Pressure at the base of the projectile, MPa.
$P_{pj}$	Projectile resistance pressure, MPa.
$P_{ps}$	Piston resistance pressure, MPa.
$P_s$	Air shock pressure ahead of the projectile, MPa.
$Q_w$	Heat loss to the gun tube walls, $\text{j/cm}^3\text{-s}$ .
$R_s$	Specific gas constant, $\text{j/g-K}$ .
$R_u$	Universal gas constant = $8.318 \text{ j/mole-K}$ .
$s_{pj}$	Projectile travel, cm.
$s_{ps}$	Piston travel, cm.
$S_2$	Chamber mass production rate times enthalpy change, $\text{j/s}$ .
$S_4$	Gun tube mass production rate times enthalpy change, $\text{j/s}$ .
$t$	Time, s.
$T_2$	Temperature in the chamber, K.

$T_4$	Average temperature in the gun tube, K.
$T_w$	Temperature of the gun tube walls, K.
$v_{12}$	Injection velocity of the liquid into the chamber, cm/s.
$v_{14}$	Injection velocity of the liquid into the gun tube, cm/s.
$v_{24}$	Injection velocity from the chamber into the gun tube, cm/s.
$v_{pj}$	Velocity of the projectile, cm/s.
$v_{ps}$	Velocity of the piston, cm/s.
$V_1$	Volume of the liquid reservoir, $\text{cm}^3$ .
$V_2$	Volume of the chamber, $\text{cm}^3$ .
$V_4$	Volume of the gun tube behind the projectile, $\text{cm}^3$ .
$V_{L2}$	Volume of the liquid in the chamber, $\text{cm}^3$ .
$V_{L4}$	Volume of the liquid in the gun tube, $\text{cm}^3$ .
$V_{G2}$	Volume of the gas in the chamber, $\text{cm}^3$ .
$V_{G4}$	Volume of the gas in the gun tube, $\text{cm}^3$ .
$x_R$	Distance from the tube end to the projectile base, cm.
$\gamma$	Ratio of specific heats.
$\epsilon_2$	Porosity of the mixture in the chamber.

- $\epsilon_4$  Porosity of the mixture in the gun tube.
- $\lambda$  Impetus of the propellant, j/g.
- $\rho_0$  Liquid density at zero pressure, g/cm<sup>3</sup>.
- $\rho_1$  Liquid density in the reservoir, g/cm<sup>3</sup>.
- $\rho_2$  Mixture density in the chamber, g/cm<sup>3</sup>.
- $\rho_4$  Mixture density in the gun tube, g/cm<sup>3</sup>.
- $\rho_{L2}$  Liquid density in the chamber, g/cm<sup>3</sup>.
- $\rho_{L4}$  Liquid density in the gun tube, g/cm<sup>3</sup>.
- $\rho_{G2}$  Gas density in the chamber, g/cm<sup>3</sup>.
- $\rho_{G4}$  Gas density in the gun tube, g/cm<sup>3</sup>.

APPENDIX A  
INPUT OPTIONS

The computer code is long (around 75 pages), so a complete listing is not given. Instead, only the description of the input options from the beginning of the code is given. A complete listing of the code (tape, disk, or hardcopy) may be obtained from the author.

```
c *****
c December 1, 1988.
c Description of input
c
c   file 1: problem title
c   80 alphanumeric characters
c   will be title on graphics files
c
c   file 2: offset, travel
c   offset = distance from end of tube to projectile (cm)
c   travel = total projectile travel (cm)
c
c   file 3:d4
c   d4 = gun tube diameter (cm)
c
c   file 4: pjwt
c   pjwt = projectile weight (g)
c
c   file 5: pswt
c   pswt = piston weight (g)
c
c   file 6: v1i,v2i
c   v1i = initial liquid reservoir volume (cm**3)
c   v2i = initial intermediate chamber volume (cm**3)
c
c   file 7: a1,a2,agres
c   a1 = area of liquid side piston face (including vents) (cm**2)
c   a2 = area of chamber side piston face (including vents) (cm**2)
c   agres = area of grease dyke (cm**2).
c
c   file 8: av12,av24
c   av12 = vent area between reservoir and chamber (cm**2).
c   av24 = vent area between chamber and tube (cm**2).
c
c   file 9: av1,av4a,av4b
c   av1 = area y vent on liquid side (cm**2)
c   av4a = area first y vent hole on tube side (cm**2)
c   av4b = area second y vent hole on tube side (cm**2)
c
c   file 10: nvo, pth
c   nvo = no. of holes between reservoir and tube.
c   total vent area = av14 * nvo.
c   av14 = min(av1, av4a+av4b)
c   pth = length of the holes (thickness of short barrel) (cm).
c
```

```

c   file 11:so1,so4a,so4b
c   so1 = piston travel to center of vent av1 (cm).
c   soa4 = distance from start of gun tube to center of av4a (cm).
c   sob4 = distance from start of gun tube to center of av4b (cm).
c
c   file 12: tpis - piston friction resistance option
c
c       if pis1 then resistance is a function of piston travel
c       file 12.1: npis
c       npis = no. of entries in piston resistance table
c       file 12.2...: sfrac(i),prs(i)
c       sfrac(i) = fraction of piston travel
c       will be normalized to max piston travel
c       prs(i) = piston resistance (MPa)
c       piston resistance is found by interpolating table
c
c   file 13: tdis - discharge coefficient option switch
c
c       if dis1 then dc function of piston travel
c       file 13.1: ndc
c       ndc = no. of table entries
c       file 13.2...: sfrac(i),dcf(i)
c       sfrac(i) = fraction of piston travel
c       will be normalized to max piston travel
c       dcf(i) = discharge coefficient
c       dc is found by interpolating table
c       dc applied to flow from reservoir to chamber and to tube.
c
c   file 14: tflux - mass flux option switch for orifice
c
c       if flux1 then steady state formulation
c       fluid entrance velocity = 0
c
c       if flux2 then unsteady mass flux formulation
c       take time derivative of mass flux
c       assume mass flux constant wrt x
c       file 14.1: fudge
c       fudge = fudge factor
c       divide time derivative of mass flux by fudge
c
c   file 15: tfluxp - mass flux option switch for tube
c
c       if flux1 then steady state formulation
c       generalized bernoulli with energy difference
c       isentropic flow
c       fluid entrance velocity = 0
c
c   file 16: tproj - projectile resistance option switch
c
c       if proj1 then projectile resistance function of proj travel
c       file 16.1: nproj
c       nproj = no. of table entries

```

```

c      file 16.2...:str(i),ptr(i)
c      str(i) = projectile travel (cm)
c      ptr(i) = resistive pressure (MPa)
c      interpolate table to find projectile resistance pressure
c
c      file 17: rh1i,rk1,rk2
c      rh1i = liquid density at zero pressure (g/cm**3)
c      rk1 = bulk modulus at zero pressure (MPa)
c      rk2 = derivative of bulk modulus
c
c      file 18: ener,gam
c      ener = chemical energy of propellant (joules/g)
c      gam = ratio of specific heats
c
c      file 19: sigma,visk
c      sigma = surface tension of propellant (dynes/cm)
c      visk = kinematic viscosity (cm**2/s)
c
c      file 20: wg,cov
c      wg = molecular weight of the gases (g/mole)
c      cov = covolume of the gas (cm**3/g)
c
c      file 21: pli,pgi
c      pli = initial liquid pressure (MPa)
c      pgi = initial gas pressure (MPa)
c
c      file 22: tdrop - droplet option switch
c
c      if drop1 then instantaneous burning
c
c      if drop2 then fixed size droplets
c      file 22.1:ddr,pbr
c      ddr = diameter of droplets (cm)
c      pbr = break pressure for change in burning rate (MPa)
c      file 22.2:adr1,bdr1
c      burning rate = adr1 * (p**dbr1)
c      if p<pbr
c      file 22.3:adr2,bdr2
c      burning rate = adr2 * (p**dbr2)
c      if p>pbr
c
c      if drop3 then fixed size droplets wrt space
c      droplet size changes with piston travel
c      file 22.1:ddr,pbr
c      ddr is ignored
c      pbr = break pressure for change in burning rate (MPa)
c      file 22.2:adr1,bdr1
c      burning rate = adr1 * (p**dbr1)
c      if p<pbr
c      file 22.3:adr2,bdr2
c      burning rate = adr2 * (p**dbr2)
c      if p>pbr

```

```

c      file 22.4:ndiam
c      ndiam = no. of table entries
c      file 22.5...:sfrac(i),diam(i)
c      sfrac(i) = fraction of piston travel
c      will be normalized to max piston travel
c      diam(i) = droplet diameter
c      the droplet diameter at any time will be found by
c      interpolating the above table
c
c      if drop4 then fixed size droplets wrt space
c      droplet size changes with projectile travel
c      file 22.1:ddr,pbr
c      ddr is ignored
c      pbr = break pressure for change in burning rate (MPa)
c      file 22.2:adr1,bdr1
c      burning rate = adr1 * (p**dbr1)
c      if p<pbr
c      file 22.3:adr2,bdr2
c      burning rate = adr2 * (p**dbr2)
c      if p>pbr
c      file 22.4:ndiam
c      ndiam = no. of table entries
c      file 22.5...:sproj(i),diam(i)
c      sproj(i) = projectile travel
c      diam(i) = droplet diameter
c      the droplet diameter at any time will be found by
c      interpolating the above table
c
c      file 23: tprim - primer option switch
c
c      if prim1 then primer instantaneously goes to gas
c
c      if prim2 set primer as liquid droplets
c      assume primer has same properties as liquid propellant
c      file 23.1: prprim
c      prprim = pressure the primer should generate
c      program computes the primer mass
c      set primer as liquid droplets in chamber/tube
c      the initial gas pressure is assumed to have been
c      by primer that has already burned
c
c      if prim3 then inject primer at a constant rate
c      assume primer has the same properties as liquid propellant,
c      except energy content may be modified.
c      inject into gun tube.
c      file 23.1: rmprim, tinjec, fener
c      rmprim = mass of primer (g)
c      tinjec = time for complete injection (s)
c      fener = factor multiplied by propellant energy content.
c
c      file 24:theat - heat loss option
c

```

```

c      if heat1 then no heat loss to the tube walls
c
c      if heat2 then convective heat loss to the gun tube
c      fits to viscosity and thermal conductivity.
c      made for HAN1845 from 1500k to 3500k.
c      file 24.1:tempw,hlfac
c      tempw = tube wall temperature (K)
c      hlfac = fudge factor
c
c      file 25: tshock
c
c      if shock1 no air shock term
c
c      if shock2 include air shock effect
c      file 25.1:airp,airt
c      airp = initial pressure in gun tube (MPa)
c      airt = initial temperature in gun tube (K)
c      file 25.2:airgam,airmw
c      airgam = ratio of specific heats of gas in barrel
c      airmw = molecular weight of gas in barrel (g/mole)
c
c      file 26: ttube
c
c      if tubel1 then standard lagrange distribution
c
c      file 27: tinc,htop
c      tinc = time increment between output lines (s)
c      htop = max time step allowed in the integration (s)
c
c      file 28: eps,srec
c      eps = error control for time integration
c      srec = cutoff between relative and absolute error control
c
c      file 29:mf,kwrite
c      mf = method of integration
c      usually mf=22 (stiff integration scheme with internally
c      generated jacobian)
c      kwrite = diagnostic
c      if kwrite=1, then print out after each time step
c
c
c      file 30:tmax
c      tmax = max run time allowed (s)
c
c      file 31:trep
c
c      if repl then integrate once
c
c      if rep2 then iterate: change vent area
c      to adjust liquid pressure
c      file 31.1: ptar, vinc
c      ptar = desired liquid pressure (MPa)

```

```

c      vinc = initial increment for changing vent area (cm**2)
c
c      file 32:tcham
c
c      if cham1 then compute chamber pressure.
c
c      if cham2 then use experimental chamber pressure.
c      read in from standard graphics file.
c      file 32.1: file1
c      file1 = file with experimental chamber pressure
c      file 32.2: kol1, kol2
c      column kol1 = time (ms).
c      column kol2 = chamber pressure (MPa).
c
c      if cham3 then use time derivative of chamber pressure.
c      integrate to get chamber pressure.
c      read in from standard graphics file.
c      file 32.1: file1
c      file1 = file with experimental chamber pressure
c      file 32.2: kol1, kol2
c      column kol1 = time (ms).
c      column kol2 = derivative of chamber pressure (MPa/s).
c *****

```

**APPENDIX B**  
**JOB STREAM FOR THE ROUND 4 MODEL**

Below is a listing of the job stream for the Round 4 model (droplet burning). Following is a listing of the output. Since there are many variables to keep track of, the output is on multiple files. Only the ones of interest for a particular problem need to be printed out. Here only the minimal output is given.

```

dr04-30mm rap-han1845-1/2 ch-y hole block-Drop4-dc=0.95-prim3
  1.88      252.6      offset  travel
  3.05      d4
 114.9      proj weight
2427.      piston weight
  84.2      36.8      v1    v2
 43.741     59.532   0.792   a1    a2    agres
  0.0      11.498     av12   av24
  .2685     .1080    .1605   av1   av4a   av4b
  12      .8687     nvo    pth
 1.633     1.93     4.30   sol   so4a   so4b
pisl      piston resistance
  2
  0.0      0.0
  1.0      0.0
disl      dis. coeff. vs. piston travel
  2      discharge coeff
  0.0      0.95
  1.0      0.95
flux1     steady state bernoulli
flux1     isentropic flow into tube
proj1     projectile resistance
  3
  0.0      65.0
  .001     5.0
 252.6     5.0
 1.45167   5600.0   9.45   rh1   k1   k2
4287.3    1.2179   energy gamma
  71.6     .06438   surface tension  kinematic viscosity
23.072    .707     mol wt gas  covolume
  1.03     .1      pl    p3
drop4     droplets
  0.01     95.2590  ddr   pbr
  1.64     .103    adr1  bdr1
  1.64     .103    adr1  bdr1
  8
  0.0      .120
  0.1      .120
  1.0      .050
  5.0      .050
 10.0     .0075
 25.0     .0075
 45.0     .0020
252.6     .0020

```

prim3  
3.00 .0015 0.70  
heat2  
300.0 1.0  
shock2  
0.1 300.  
1.4 28.84  
tubel  
5.00e-05 1.00e-05  
1.00e-06 1.00e-09  
22 0  
80.0  
repl  
cham1

inject primer  
rmprim tinjec  
heat loss to walls  
tube temp fudge factor  
air shock  
airp airt  
airgam airmw  
standard lagrange distribution  
tinc htop  
eps srec  
mf kwrite  
tmax  
integrate once  
compute p2

date: 12-09-88 time: 14:44:42

dr04-30mm rep-hen1845-1/2 ch-y hole block-Drop4-dc=0.95-prim3

offset = 1.8800 travel = 252.60  
tube diam = 3.0500 tube area = 7.3062  
pjwt = 114.90 pswt = 2427.0  
v1 in = 84.200 v2 in = 36.800  
a1 = 43.741 a2 = 59.532 agres = 0.79200

max piston travel = 1.9250

av12 = 0.00000 av24 = 11.498  
av1 = 0.26850 rad = 0.29234  
av4a = 0.10800 rad = 0.18541  
av4b = 0.16050 rad = 0.22602

nvo = 12 pth = 0.86870

so1 = 1.6330 so4a = 1.9300 so4b = 4.3000

hydraulic diff = 1.3429

pis1 piston resistance

npis = 2

frac pis trav = 0.00000 pis trav = 0.00000 pis resistance = 0.00000  
frac pis trav = 1.00000 pis trav = 1.9250 pis resistance = 0.00000

dis1 dis. coeff. vs. piston travel

ndc = 2

frac pis trav = 0.00000 pis trav = 0.00000 dis coeff = 0.95000  
frac pis trav = 1.00000 pis trav = 1.9250 dis coeff = 0.95000

flux1 steady state bernoulli

```

flux1          isentropic flow into tube

proj1          projectile resistance

nproj = 3

travel = 0.00000      resistive press = 65.000
travel = 1.00000E-03  resistive press = 5.0000
travel = 252.60       resistive press = 5.0000

dens liquid = 1.4517      k1 = 5600.0      k2 = 9.4500

chem energy = 4287.3      gam = 1.2179

surface tension = 71.600  kinematic viscosity = 6.43800E-02

mol wt gas = 23.072      covolume = 0.70700

pres liquid = 1.0300     pres gas = 0.10000

specific gas constant = 0.36036

cv = 1.6538             cp = 2.0142

drop4          droplets

ddr = 1.00000E-02      pbr = 95.259
adr1 = 1.6400         bdr1 = 0.10300
adr2 = 1.6400         bdr2 = 0.10300
ndiam = 8

s proj = 0.00000      drop diam = 0.12000
s proj = 0.10000     drop diam = 0.12000
s proj = 1.00000     drop diam = 5.00000E-02
s proj = 5.00000     drop diam = 5.00000E-02
s proj = 10.000      drop diam = 7.50000E-03
s proj = 25.000      drop diam = 7.50000E-03
s proj = 45.000      drop diam = 2.00000E-03
s proj = 252.60      drop diam = 2.00000E-03

prim3          inject primer

```

mass primer = 3.0000  
time for injection = 1.50000E-03  
rate of injection = 2000.0  
multiply energy content by 0.70000

heat2            heat loss to walls  
tube temperature = 300.00  
heat loss fudge factor = 1.0000

shock2            air shock  
airp = 0.10000    airt = 300.00  
airgam = 1.4000    airmw = 28.840

tube1            standard lagrange distribution  
tinc = 5.00000E-05    htop = 1.00000E-05  
mf = 22    eps = 1.00000E-06    srec = 1.00000E-09  
tmax = 80.000

rep1            integrate once  
cham1            compute p2

charge = 122.25    primer = 3.0355    c/m = 1.0640  
initial gas volume = 50.536  
initial total volume = 134.74  
loading density = 0.90735  
total mass = 125.29  
total energy = 0.53316E+06

t ms	p1	p2	pl	ph	p4	pr	s ps	v ps	s pj	v pj
0.000	1.030	0.100	0.100	0.100	0.100	0.100	0.000	0.000	0.000	0.000
0.050	0.677	1.200	1.927	1.927	1.927	1.927	0.000	1.814	0.000	0.000
0.100	1.868	2.652	2.817	2.817	2.817	2.817	0.000	15.655	0.000	0.000
0.150	4.304	3.963	4.085	4.085	4.085	4.085	0.002	26.909	0.000	0.000
0.200	5.923	5.269	5.386	5.386	5.386	5.386	0.003	36.789	0.000	0.000
0.250	7.703	6.582	6.694	6.694	6.694	6.694	0.005	47.220	0.000	0.000
0.300	9.618	7.904	8.012	8.012	8.012	8.012	0.008	56.893	0.000	0.000
0.350	11.595	9.237	9.342	9.342	9.342	9.342	0.011	65.036	0.000	0.000
0.400	13.568	10.584	10.687	10.687	10.687	10.687	0.014	71.561	0.000	0.000
0.450	15.507	11.949	12.049	12.049	12.049	12.049	0.018	76.855	0.000	0.000
0.500	17.420	13.332	13.429	13.429	13.429	13.429	0.022	81.424	0.000	0.000
0.550	19.329	14.734	14.829	14.829	14.829	14.829	0.026	85.649	0.000	0.000
0.600	21.254	16.158	16.251	16.251	16.251	16.251	0.031	89.714	0.000	0.000
0.650	23.209	17.605	17.695	17.695	17.695	17.695	0.035	93.668	0.000	0.000
0.700	25.196	19.075	19.163	19.163	19.163	19.163	0.040	97.508	0.000	0.000
0.750	27.215	20.569	20.656	20.656	20.656	20.656	0.045	101.235	0.000	0.000
0.800	29.266	22.089	22.175	22.175	22.175	22.175	0.050	104.861	0.000	0.000
0.850	31.351	23.636	23.720	23.720	23.720	23.720	0.055	108.405	0.000	0.000
0.900	33.472	25.210	25.293	25.293	25.293	25.293	0.061	111.884	0.000	0.000
0.950	35.630	26.813	26.895	26.895	26.895	26.895	0.067	115.309	0.000	0.000
1.000	37.926	28.445	28.526	28.526	28.526	28.526	0.072	118.684	0.000	0.000
1.050	40.063	30.107	30.188	30.188	30.188	30.188	0.078	122.016	0.000	0.000
1.100	42.341	31.800	31.881	31.881	31.881	31.881	0.085	125.309	0.000	0.000
1.150	44.661	33.525	33.606	33.606	33.606	33.606	0.091	128.568	0.000	0.000
1.200	47.025	35.283	35.363	35.363	35.363	35.363	0.097	131.798	0.000	0.000
1.250	49.433	37.074	37.154	37.154	37.154	37.154	0.104	135.002	0.000	0.000
1.300	51.886	38.899	38.979	38.979	38.979	38.979	0.111	138.183	0.000	0.000
1.350	54.386	40.759	40.839	40.839	40.839	40.839	0.118	141.342	0.000	0.000
1.400	56.932	42.654	42.734	42.734	42.734	42.734	0.125	144.483	0.000	0.000
1.450	59.527	44.585	44.665	44.665	44.665	44.665	0.132	147.607	0.000	0.000
1.500	62.171	46.553	46.633	46.633	46.633	46.633	0.140	150.715	0.000	0.000
1.550	64.147	47.252	47.263	47.263	47.263	47.263	0.147	148.094	0.000	0.000
1.600	64.824	48.002	48.015	48.015	48.015	48.015	0.155	142.599	0.000	0.000
1.650	65.225	48.800	48.814	48.814	48.814	48.814	0.162	142.553	0.000	0.000
1.700	66.172	49.628	49.644	49.644	49.644	49.644	0.169	146.524	0.000	0.000
1.750	67.562	50.488	50.506	50.506	50.506	50.506	0.176	149.848	0.000	0.000
1.800	68.955	51.387	51.408	51.408	51.408	51.408	0.184	151.001	0.000	0.000
1.850	70.190	52.330	52.353	52.353	52.353	52.353	0.191	151.489	0.000	0.000
1.900	71.405	53.314	53.339	53.339	53.339	53.339	0.199	152.746	0.000	0.000
1.950	72.740	54.337	54.363	54.363	54.363	54.363	0.207	154.713	0.000	0.000

t ms	p1	p2	pl	ph	p4	pr	s ps	v ps	s pj	v pj
2.000	74.194	55.397	55.426	55.426	55.426	55.426	0.215	156.665	0.000	0.000
2.050	75.698	56.496	56.527	56.527	56.527	56.527	0.222	158.306	0.000	0.000
2.100	77.222	57.636	57.668	57.668	57.668	57.668	0.230	159.853	0.000	0.000
2.150	78.786	58.815	58.849	58.849	58.849	58.849	0.238	161.544	0.000	0.000
2.200	80.413	60.034	60.069	60.069	60.069	60.069	0.246	163.377	0.000	0.000
2.250	82.104	61.291	61.328	61.328	61.328	61.328	0.255	165.230	0.000	0.000
2.300	83.848	62.588	62.627	62.627	62.627	62.627	0.263	167.054	0.000	0.000
2.350	85.639	63.924	63.964	63.964	63.964	63.964	0.271	168.888	0.000	0.000
2.400	87.480	65.301	65.343	65.330	65.339	65.331	0.280	170.768	0.000	0.812
2.450	87.858	66.671	66.688	64.653	66.033	64.723	0.289	176.143	0.016	1089.676
2.500	79.275	67.173	67.173	65.180	66.461	65.036	0.298	227.173	0.118	2992.586
2.550	75.107	66.671	66.669	64.837	65.879	64.299	0.313	355.524	0.315	4888.780
2.600	80.818	65.489	65.487	63.899	64.609	62.852	0.333	453.116	0.606	6747.792
2.650	84.645	64.636	64.635	63.299	63.651	61.681	0.357	491.857	0.989	8561.751
2.700	86.240	64.289	64.287	63.183	63.183	60.977	0.382	500.918	1.462	10349.210
2.750	86.030	63.551	63.542	62.650	62.326	59.893	0.407	497.507	2.024	12107.619
2.800	66.945	62.697	62.686	61.961	61.342	58.652	0.432	547.243	2.672	13828.136
2.850	67.811	61.335	61.330	60.747	59.871	56.954	0.463	693.018	3.406	15501.999
2.900	69.095	59.873	59.872	59.397	58.288	55.119	0.501	809.361	4.222	17118.824
2.950	70.067	58.462	58.464	58.072	56.747	53.312	0.544	897.979	5.117	18676.987
3.000	71.120	57.633	57.682	57.354	55.821	52.099	0.590	963.728	6.088	20184.517
3.050	72.984	57.964	58.166	57.886	56.131	52.063	0.640	1013.316	7.135	21670.631
3.100	76.560	60.159	60.750	60.503	58.476	53.928	0.692	1053.600	8.256	23182.539
3.150	84.352	66.312	68.070	67.836	65.379	59.999	0.745	1092.712	9.455	24809.030
3.200	103.615	83.190	86.359	86.112	82.829	75.769	0.801	1146.326	10.743	26790.694
3.250	123.098	101.122	102.175	101.926	97.794	89.030	0.861	1243.993	12.142	29248.725
3.300	141.655	115.243	115.822	115.577	110.501	99.858	0.926	1362.143	13.674	32089.808
3.350	158.097	126.572	127.014	126.777	120.719	108.130	0.997	1475.451	15.356	35232.916
3.400	172.116	135.637	136.027	135.804	128.747	114.187	1.073	1574.388	17.201	38601.653
3.450	183.711	142.826	143.193	142.986	134.931	118.407	1.154	1655.975	19.219	42131.509
3.500	193.037	148.456	148.810	148.620	139.583	121.129	1.238	1720.736	21.416	45769.461
3.550	200.340	152.787	153.129	152.957	142.967	122.643	1.326	1770.814	23.797	49472.490
3.600	212.305	156.224	156.596	156.440	145.528	123.392	1.415	1791.504	26.364	53207.117
3.650	232.887	160.230	160.632	160.492	148.627	124.618	1.503	1703.052	29.118	56969.281
3.700	253.929	165.155	165.468	165.342	152.509	126.591	1.583	1474.099	32.061	60780.087
3.750	265.583	170.897	171.056	170.943	157.155	129.352	1.649	1156.237	35.197	64664.077
3.800	266.554	177.241	177.296	177.195	162.480	132.847	1.699	859.659	38.529	68645.444
3.850	266.396	184.193	184.211	184.120	168.491	137.049	1.736	647.006	42.064	72746.469
3.900	270.857	192.028	192.028	191.946	175.374	142.066	1.765	506.047	45.807	76992.590
3.950	271.450	194.498	194.309	194.237	177.201	142.987	1.787	401.145	49.765	81345.899

t ms	p1	p2	pl	ph	p4	pr	s ps	v ps	s pj	v pj
4.000	264.473	191.129	190.645	190.584	173.617	139.563	1.805	320.268	53.940	85649.723
4.050	253.535	184.354	183.618	183.567	167.001	133.765	1.820	258.629	58.327	89799.671
4.100	240.632	175.765	174.852	174.809	158.839	126.812	1.832	211.349	62.917	93747.223
4.150	226.995	166.369	165.347	165.312	150.045	119.441	1.841	174.743	67.698	97450.391
4.200	213.366	156.786	155.712	155.683	141.169	112.084	1.849	146.095	72.658	100921.474
4.250	200.169	147.387	146.301	146.276	132.530	104.988	1.856	123.421	77.786	104159.339
4.300	187.636	138.380	137.311	137.291	124.300	98.280	1.862	105.275	83.070	107174.648
4.350	175.877	129.875	128.841	128.824	116.566	92.017	1.866	90.598	88.500	109980.920
4.400	164.927	121.916	120.930	120.916	109.359	86.216	1.871	78.605	94.065	112592.773
4.450	154.780	114.514	113.582	113.570	102.676	80.866	1.874	68.711	99.756	115024.883
4.500	145.402	107.652	106.777	106.767	96.500	75.945	1.878	60.476	105.565	117291.406
4.550	136.748	101.306	100.488	100.480	90.801	71.425	1.880	53.564	111.483	119405.664
4.600	128.766	95.442	94.680	94.673	85.545	67.274	1.883	47.717	117.503	121380.015
4.650	121.404	90.024	89.317	89.311	80.698	63.462	1.885	42.737	123.619	123225.808
4.700	114.611	85.018	84.362	84.357	76.227	59.957	1.887	38.465	129.823	124953.406
4.750	108.335	80.389	79.781	79.777	72.098	56.731	1.889	34.777	136.112	126572.237
4.800	102.534	76.105	75.542	75.538	68.281	53.759	1.891	31.577	142.479	128090.859
4.850	97.162	72.137	71.615	71.612	64.749	51.017	1.892	28.784	148.920	129517.034
4.900	92.184	68.455	67.972	67.969	61.476	48.483	1.894	26.331	155.429	130857.801
4.950	87.564	65.037	64.589	64.586	58.438	46.137	1.895	24.171	162.004	132119.544
5.000	83.269	61.858	61.442	61.440	55.616	43.963	1.896	22.258	168.640	133308.057
5.050	79.272	58.898	58.512	58.510	52.990	41.945	1.897	20.557	175.334	134428.607
5.100	75.547	56.138	55.779	55.778	50.542	40.068	1.898	19.038	182.082	135485.985
5.150	72.070	53.561	53.228	53.226	48.259	38.321	1.899	17.678	188.881	136484.555
5.200	68.821	51.152	50.841	50.840	46.125	36.691	1.900	16.454	195.729	137428.298
5.250	65.780	48.897	48.607	48.606	44.128	35.169	1.901	15.351	202.623	138320.853
5.300	62.930	46.783	46.513	46.512	42.257	33.746	1.901	14.352	209.561	139165.548
5.350	60.257	44.799	44.547	44.546	40.503	32.413	1.902	13.446	216.539	139965.435
5.400	57.745	42.935	42.700	42.699	38.854	31.163	1.903	12.621	223.557	140723.314
5.450	55.383	41.182	40.962	40.961	37.304	29.989	1.903	11.869	230.611	141441.760
5.500	53.159	39.531	39.324	39.324	35.845	28.885	1.904	11.180	237.700	142123.142
5.550	51.062	37.974	37.780	37.779	34.469	27.847	1.904	10.549	244.823	142769.648
5.600	49.083	36.504	36.322	36.322	33.171	26.868	1.905	9.969	251.976	143383.295
5.604	48.916	36.380	36.827	36.827	33.061	25.530	1.905	9.921	252.600	143435.165

muzzle vel (m/s) 1434.4  
max v p1s (m/s) 17.9  
max p1 (MPa) 271.4  
max p2 (MPa) 194.5  
max p1 (MPa) 194.3  
max pr (MPa) 177.2  
max acc (k-g) 88.7  
max mass error 0.01  
max energy error 0.52  
ballistic efficiency = 22.55 %  
expansion ratio = 14.92  
loss to tube walls = 11.67 %  
run time = 6.2 nstep = 1514

max	time	s ps	v ps	s pj	v pj	acc	p1	p2	pl	p4	pr	z bur
p1	3.95	0.018	4.01	0.498	813.5	88.67	271.4	194.5	194.3	177.2	143.0	0.80
p2	3.95	0.018	4.01	0.498	813.5	88.67	271.4	194.5	194.3	177.2	143.0	0.80
pl	3.95	0.018	4.01	0.498	813.5	88.67	271.4	194.5	194.3	177.2	143.0	0.80
p4	3.95	0.018	4.01	0.498	813.5	88.67	271.4	194.5	194.3	177.2	143.0	0.80
pr	3.95	0.018	4.01	0.498	813.5	88.67	271.4	194.5	194.3	177.2	143.0	0.80
v ps	3.60	0.014	17.92	0.264	532.1	76.32	212.3	156.2	156.6	145.5	123.4	0.39
burn	0.00	0.000,	0.00	0.000	0.0	0.00	0.0	0.0	0.0	0.0	0.0	0.00
muz	5.60	0.019	0.10	2.526	1434.4	14.55	48.9	36.4	36.8	33.1	25.5	0.99

APPENDIX C  
JOB STREAM FOR THE ROUND 25 MODEL

Below is a listing of the job stream for the Round 25 model (droplet burning). Following is the summary page from the output.

```

dr25-30mm rap-han1845-1/2 ch-stag hole-Drop-dc=0.95-prim3
  1.96      252.6      offset travel
  3.05
  350.0      d4
2427.      proj weight
      piston weight
  84.2      36.8      v1 v2
  43.741    59.532    0.792    a1 a2 agres
  0.0      11.498      av12 av24
  .1366    .0401    .0965    av1 av4a av4b
  12      .8687      nvo pth
  1.716    1.93      4.30    sol so4a so4b
pisl      piston resistance
  2
  0.0      0.0
  1.0      0.0
disl      dis. coeff. vs. piston travel
  2      discharge coeff
  0.0      0.95
  1.0      0.95
flux1     steady state bernoulli
flux1     isentropic flow into tube
proj1     projectile resistance
  3
  0.0      45.0
  .001      5.0
  252.6     5.0
  1.45167   5600.0   9.45    rh1 k1 k2
  4287.3    1.2179   energy gamma
  71.6      .06438   surface tension kinematic viscosity
  23.072    .707     mol wt gas covolume
  1.03      .1       pl p3
drop4     droplets
  0.01     95.2590  ddr pbr
  1.64     .103     adr1 bdr1
  1.64     .103     adr1 bdr1
  7
  0.0      .090
  0.01     .090
  0.1      .025
  1.0      .020
  4.0      .0125
  5.0      .005
  252.6    .005
prim3     inject primer
  2.50     .002     0.70    rmprim tinjec
heat2     heat loss to walls
  300.0    1.0      tube temp fudge factor

```

shock2			air shock	
0.1	300.		airp	airt
1.4	28.84		airgam	airmw
tubel			standard	lagrange distribution
5.00e-05	1.00e-05		tinc	htop
1.00e-06	1.00e-09		eps	srec
22	0		mf	kwrite
80.0			tmax	
repl			integrate	once
cham1			compute	p2

muzzle vel (m/s)	913.9		
max v pis (m/s)	10.5		
max p1 (MPa)	258.6		
max p2 (MPa)	192.5		
max pl (MPa)	192.7		
max pr (MPa)	188.7		
max acc (k-g)	37.4		
max mass error	0.00		
max energy error	0.29		
ballistic efficiency =	27.89 %		
expansion ratio =	14.86		
loss to tube walls =	11.99 %		
run time =	6.2	nstep =	1591

DISTRIBUTION LIST

<u>No. of Copies</u>	<u>Organization</u>	<u>No. of Copies</u>	<u>Organization</u>
12	Administrator Defense Technical Info Center ATTN: DTIC-DDA Cameron Station Alexandria, VA 22304-6145	5	Commander US Army Armament, Rsch, Development & Engr Center ATTN: SMCAR-FSS-DA, Bldg 94 C. Daly R. Kopmann J. Irizarry M. Oetken N. Kendl Picatinny Arsenal, NJ 07806-5000
2	Director Defense Advanced Research Projects Agency ATTN: J. Lupo J. Richardson 1400 Wilson Boulevard Arlington, VA 22209	5	Director Benet Weapons Laboratory US Army Armament, Rsch, Development & Engr Center ATTN: SMCAR-CCB-DS, E. Conroy A. Graham SMCAR-CCB, L. Johnson SMCAR-CCB-S, F. Heiser SMCAR-LCB-TL Watervliet, NY 12189-4050
2	HQDA (SARD-TR/B. Zimmerman, I. Szkrybalo) Washington, DC 20310-0001	1	Commander US Army Armament, Munitions and Chemical Command ATTN: SMCAR-ESP-L Rock Island, IL 61299-5000
1	Commander US Army Materiel Command ATTN: AMCDRA-ST 5001 Eisenhower Avenue Alexandria, VA 22333-0001	1	Commander US Army Aviation Systems Cmd ATTN: AMSAV-DACL 4300 Goodfellow Blvd St. Louis, MO 63120-1798
1	HQ, US Army Materiel Command ATTN: AMCICP-AD, B. Dunetz 5001 Eisenhower Avenue Alexandria, VA 22333-0001	1	Commander Materials Technology Lab US Army Laboratory Cmd ATTN: SLCMT-MCM-SB M. Levy Watertown, MA 02172-0001
14	Cmdr, US Army Armament, Rsch, Development & Engr Center ATTN: SMCAR-TSS SMCAR-TDC (2 COPIES) SMCAR-MSI (2 COPIES) SMCAR-AEE-BR, B. Brodman SMCAR-AEE-B, D. Downs SMCAR-AEE-BR, W. Seals A. Beardell SMCAR-AEE-W, N. Slagg SMCAR-AEE, A. Bracuti J. Lannon SMCAR-FSS-D, L. Frauen SMCAR-FSA-S, H. Liberman Picatinny Arsenal, NJ07806-5000		

DISTRIBUTION LIST

<u>No. of</u> <u>Copies</u>	<u>Organization</u>	<u>No. of</u> <u>Copies</u>	<u>Organization</u>
1	Director US Army Aviation Rsch and Technology Activity Ames Research Center Moffett Field, CA 94035-1099	1	Commander US Army Tank Automotive Cmd ATTN: AMSTA-TSL Warren, MI 48397-5000
1	Commander US Army Communications Electronics Command ATTN: AMSEL-ED Fort Monmouth, NJ 07703-5022	1	Director US Army Laboratory Cmd Army Research Office ATTN: Tech Library PO Box 12211 Research Triangle Park, NC 27709-2211
1	Commander ERADCOM Technical Library ATTN: STET-L Ft. Monmouth, NJ 07703-5301	1	Director TRADOC Analysis Command ATTN: ATAA-SL White Sands Missile Range NM 88002-5502
2	Commander US Army Laboratory Cmd ATTN: SLCHD-TA-L AMSLC-DL 2800 Powder Mill Rd Adelphi, MD 20783-1145	1	Commandant US Army Infantry School ATTN: ATSH-CD-CSO-OR Fort Benning, GA 31905-5660
1	Commander US Army Missile Command ATTN: AMSMI-RD Redstone Arsenal, AL 35898-5000	1	Commander US Army Armament, Rsch, Development and Engr Center ATTN: SMCAR-CCS-C, T Hung Picatinny Arsenal, NJ 07806-5000
1	Commander US Army Missile Command ATTN: AMSMI-AS Redstone Arsenal, AL 35898-5000	2	Commandant US Army Field Artillery School ATTN: ATSF-CMW ATSF-TSM-CN, J. Spicer Fort Sill, OK 73503
1	Commander US Army Belvoir RD&E Ctr ATTN: STRBE-WC Tech Library (Vault) B-315 Fort Belvoir, VA 22060-5606	1	Commandant US Army Armor Center ATTN: ATSB-CD-MLD Fort Knox, KY 40121

DISTRIBUTION LIST

<u>No. of</u> <u>Copies</u>	<u>Organization</u>	<u>No. of</u> <u>Copies</u>	<u>Organization</u>
1	Commander Naval Surface Weapons Center ATTN: D.A. Wilson, Code G31 Dahlgren, VA 22448-5000	1	Commandant USAFAS ATTN: ATSF-TSM-CN Fort Sill, OK 73503-5600
1	Commander Naval Surface Weapons Center ATTN: J. East, Code G33 Dahlgren, VA 22448-5000	1	Director Jet Propulsion Lab ATTN: Tech Library 4800 Oak Grove Drive Pasadena, CA 91109
2	Commander US Naval Surface Weapons Ctr ATTN: O. Dengel K. Thorsted Silver Spring, MD 20902-5000	2	Director National Aeronautics and Space Administration ATTN: MS-603, Tech Lib MS-86, Dr. Povinelli 21000 Brookpark Road Lewis Research Center Cleveland, OH 44135
1	Commander Naval Weapons Center China Lake, CA 93555-6001		
1	Commander Naval Ordnance Station ATTN: C. Dale Code 5251 Indian Head, MD 20640	1	Director National Aeronautics and Space Administration Manned Spacecraft Center Houston, TX 77058
1	Superintendent Naval Postgraduate School Dept of Mechanical Engr ATTN: Code 1424, Library Monterey, CA 93943	10	Central Intelligence Agency Office of Central Reference Dissemination Branch Room GE-47 HQS Washington, DC 20502
1	AFWL/SUL Kirtland AFB, NM 87117-5800	1	Central Intelligence Agency ATTN: Joseph E. Backofen HQ Room 5F22 Washington, DC 20505
1	Air Force Armament Lab ATTN: AFATL/DLODL Eglin AFB, FL 32542-5000	3	Bell Aerospace Textron ATTN: F. Boorady F. Picirillo A.J. Friona PO Box One Buffalo, NY 14240
1	AFOSR/NA (L. Caveny) Bldg 410 Bolling AFB, DC 20332		

DISTRIBUTION LIST

<u>No. of Copies</u>	<u>Organization</u>	<u>No. of Copies</u>	<u>Organization</u>
1	Calspan Corporation ATTN: Tech Library PO Box 400 Buffalo, NY 14225	1	Safety Consulting Engr ATTN: Mr. C. James Dahn 5240 Pearl St Rosemont, IL 60018
8	General Electric Ord Sys Div ATTN: J. Mandzy, OP43-220 R.E. Mayer H. West W. Pasko R. Pate I. Magoon J. Scudiere Minh Luu 100 Plastics Avenue Pittsfield, MA 01201-3698	1	Science Applications, Inc. ATTN: R. Edelman 23146 Cumorah Crest Woodland Hills, CA 91364
		2	Science Applications Int'l Corporation ATTN: Dr. F. T. Phillips Dr. Fred Su 10210 Campus Point Drive San Diego, CA 92121
1	General Electric Company Armament Systems Department ATTN: D. Maher Burlington, VT 05401	1	Science Applications Int'l Corporation ATTN: Norman Banks 4900 Waters Edge Drive Suite 255 Raleigh, NC 27606
1	IITRI ATTN: Library 10 W. 35th St Chicago, IL 60616	1	Sundstrand Aviation Operations ATTN: Mr. Owen Briles PO Box 7202 Rockford, IL 61125
1	Olin Chemicals Research ATTN: David Gavin PO Box 586 Cheshire, CT 06410-0586	1	Veritay Technology, Inc. ATTN: E.B. Fisher 4845 Millersport Highway PO Box 305 East Amherst, NY 14051-0305
2	Olin Corporation ATTN: Victor A. Corso Dr. Ronald L. Dotson PO Box 30-9644 New Haven, CT 06536	1	Director Applied Physics Laboratory The Johns Hopkins Univ. Johns Hopkins Road Laurel, MD 20707
1	Paul Gough Associates ATTN: Paul Gough PO Box 1614 Portsmouth, NH 03801		

DISTRIBUTION LIST

<u>No. of Copies</u>	<u>Organization</u>	<u>No. of Copies</u>	<u>Organization</u>
2	Director CPIA The Johns Hopkins Univ. ATTN: T. Christian Tech Library Johns Hopkins Road Laurel, MD 20707	2	Princeton Combustion Rsch Laboratories, Inc. ATTN: N.A. Messina M. Summerfield 4275 US Highway One North Monmouth Junction, NJ 08852
1	U. of Illinois at Chicago ATTN: Professor Sohail Murad Dept of Chemical Engr Box 4348 Chicago, IL 60680	1	University of Arkansas Dept of Chemical Engr ATTN: J. Havens 227 Engineering Building Fayetteville, AR 72701
1	U. of MD at College Park ATTN: Professor Franz Kasler Department of Chemistry College Park, MD 20742	3	University of Delaware Department of Chemistry ATTN: Mr. James Cronin Professor Thomas Brill Mr. Peter Spohn Newark, DE 19711
1	U. of Missouri at Columbia ATTN: Professor R. Thompson Department of Chemistry Columbia, MO 65211	1	U. of Texas at Austin Bureau of Engineering Rsch ATTN: BRC EME133, Room 1.100 H. Fair 10100 Burnet Road Austin, TX 78758
1	U. of Michigan ATTN: Prof. Gerard M. Faeth Dept of Aerospace Engr Ann Arbor, MI 48109-3796		
1	U. of Missouri at Columbia ATTN: Professor F.K. Ross Research Reactor Columbia, MO 65211		
1	U. of Missouri at Kansas City Department of Physics ATTN: Prof. R.D. Murphy 1110 East 48th Street Kansas City, MO 64110-2499		<u>Aberdeen Proving Ground</u>  Dir, USAMSAA ATTN: AMXSY-D AMXSY-MP, H. Cohen
1	Pennsylvania State University Dept of Mechanical Engr ATTN: Prof. K. Kuo University Park, PA 16802		Cdr, USATECOM ATTN: AMSTE-TO-F

DISTRIBUTION LIST

<u>No. of Copies</u>	<u>Organization</u>	<u>No. of Copies</u>	<u>Organization</u>
3	Cdr, CRDEC, AMCCOM ATTN: SMCCR-RSP-A SMCCR-MU SMCCR-SPS-IL		

DISTRIBUTION LIST

No. of  
Copies

Organization

1

Dr. Clive Woodley  
GS2 Division  
Building R31  
RARDE  
Ft. Halstead  
Sevenoaks, Kent TN14 7BT  
England

USER EVALUATION SHEET/CHANGE OF ADDRESS

This laboratory undertakes a continuing effort to improve the quality of the reports it publishes. Your comments/answers below will aid us in our efforts.

1. Does this report satisfy a need? (Comment on purpose, related project, or other area of interest for which the report will be used.) \_\_\_\_\_  
\_\_\_\_\_
2. How, specifically, is the report being used? (Information source, design data, procedure, source of ideas, etc.) \_\_\_\_\_  
\_\_\_\_\_
3. Has the information in this report led to any quantitative savings as far as man-hours or dollars saved, operating costs avoided, or efficiencies achieved, etc? If so, please elaborate. \_\_\_\_\_  
\_\_\_\_\_
4. General Comments. What do you think should be changed to improve future reports? (Indicate changes to organization, technical content, format, etc.) \_\_\_\_\_  
\_\_\_\_\_

BRL Report Number \_\_\_\_\_ Division Symbol \_\_\_\_\_

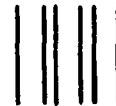
Check here if desire to be removed from distribution list. \_\_\_\_\_

Check here for address change. \_\_\_\_\_

Current address: Organization \_\_\_\_\_  
Address \_\_\_\_\_  
\_\_\_\_\_

-----FOLD AND TAPE CLOSED-----

Director  
U.S. Army Ballistic Research Laboratory  
ATTN: SLCBR-DD-T (NEI)  
Aberdeen Proving Ground, MD 21005-5066



NO POSTAGE  
NECESSARY  
IF MAILED  
IN THE  
UNITED STATES

OFFICIAL BUSINESS  
PENALTY FOR PRIVATE USE \$300

**BUSINESS REPLY LABEL**  
FIRST CLASS PERMIT NO. 12062 WASHINGTON D. C.

POSTAGE WILL BE PAID BY DEPARTMENT OF THE ARMY



Director  
U.S. Army Ballistic Research Laboratory  
ATTN: SLCBR-DD-T (NEI)  
Aberdeen Proving Ground, MD 21005-9989